European Journal of Medicinal Chemistry 163 (2019) 67–82

Contents lists available at ScienceDirect

European Journal of Medicinal Chemistry

journal homepage: http://www.elsevier.com/locate/ejmech

Research paper

Synthesis and mechanistic studies of diketo acids and their bioisosteres as potential antibacterial agents

Phool Hasan [a, b], Vijay K. Pillalamarri [c], Babita Aneja [a], Mohammad Irfan [a], Mudsser Azam [d], Ahmad Perwez [e], Ronan Maguire [f], Umesh Yadava [g], Kevin Kavanagh [f], Constantin G. Daniliuc [h], Md Belal Ahmad [b], M. Moshahid A. Rizvi [e], Qazi Mohd Rizwanul Haq [d], Anthony Addlagatta [c], Mohammad Abid [a, *]

[a] Medicinal Chemistry Laboratory, Department of Biosciences, Jamia Millia Islamia, Jamia Nagar, New Delhi, 110025, India
[b] Department of Chemistry, TNB College, TM Bhagalpur University, Bhagalpur, 812007, India
[c] Centre for Chemical Biology, Indian Institute of Chemical Technology, Tarnaka, Hyderabad, 500607, India
[d] Microbiology Research Laboratory, Department of Biosciences, Jamia Millia Islamia, Jamia Nagar, New Delhi, 110025, India
[e] Genome Biology Laboratory, Department of Biosciences, Jamia Millia Islamia, Jamia Nagar, New Delhi, 110025, India
[f] Department of Biology, Maynooth University, Co. Kildare, W23 F2H6, Ireland
[g] Department of Physics, Deen Dayal Upadhyay Gorakhpur University, Gorakhpur, Uttar Pradesh, 273009, India
[h] Organisch-Chemisches Institut, Westfälische Wilhelm-Universität, Münster, Germany

ARTICLE INFO

Article history:
Received 13 July 2018
Received in revised form
13 October 2018
Accepted 21 November 2018
Available online 22 November 2018

Keywords:
Diketo acids
Bioisosteres
Cytotoxicity
Methionine aminopeptidase
Antibacterial
Galleria mellonella

ABSTRACT

A series of diketo esters and their pertinent bioisosteres were designed and synthesized as potent antibacterial agents by targeting methionine amino peptidases (MetAPs). In the biochemical assay against purified MetAPs from *Streptococcus pneumoniae* (*Sp*MetAP1a), *Mycobacterium tuberculosis* (*Mt*MetAP1c), *Enterococcus faecalis* (*Ef*MetAP1a) and human (*Hs*MetAP1b), compounds **3a**, **4a** and **5a** showed more than 85% inhibition of all the tested MetAPs at 100 μM concentration. Compounds **4a** and **5a** also exhibited antibacterial potential with MIC values 62.5 μg/mL (*S. pneumoniae*), 31.25 μg/mL (*E. faecalis*), 62.5 μg/mL (*Escherichia coli*) and 62.5 μg/mL (*S. pneumoniae*), 62.5 μg/mL (*E. coli*), respectively. Moreover, **5a** also significantly inhibited the growth of multidrug resistant *E. coli* strains at 512 μg/mL conc., while showing no cytotoxic effect towards healthy CHO cells and thus being selected. Growth kinetics study showed significant inhibition of bacterial growth when treated with different conc. of **5a**. TEM analysis also displayed vital damage to bacterial cells by **5a** at MIC conc. Moreover, significant inhibition of biofilm formation was observed in bacterial cells treated with MIC conc. of **5a** as visualized by SEM micrographs. Interestingly, **5a** did not cause an alteration in the hemocyte density in *Galleria mellonella* larvae which is considered *in vivo* model for antimicrobial studies and was non-toxic up to a conc. of 2.5 mg/mL.

1. Introduction

Increase in consumption of antibiotics due to the emergence of dangerous and multidrug resistant strains has become a serious worldwide medical crisis in recent decades [1,2]. India leads in consumption of antibiotics, expressed in defined daily doses (DDDs), among low middle income countries (LMICs) with 103% rise from 2000 to 2015 [2]. Recent reports from the Centre for Disease Control and Prevention (CDC) suggested that multi-drug resistant bacterial strains are affecting at least 2 million people and are responsible for approximately 23,000 deaths each year in the United States alone [3]. This escalating evolution of resistance coupled with a diminished antibiotic pipeline has increased the urgency of the search for new antibiotics and enzyme targets [4]. In an attempt to identify potent inhibitors against bacterial infections, we have directed our drug-discovery approach towards methionine aminopeptidase (MetAP) which is crucial for the viability of bacterial cells [5].

MetAPs are ubiquitous metalloproteases present in prokaryotic and eukaryotic cells [6]. This enzyme cleaves the initiated

* Corresponding author.
E-mail address: mabid@jmi.ac.in (M. Abid).

https://doi.org/10.1016/j.ejmech.2018.11.053
0223-5234/

methionine from the newly synthesized proteins, co-translationally [7,8]. MetAPs are typically classified into two types, type I (MetAP1) and type II (MetAP2), differentiated by the presence of a 60 amino acid insert in the latter. MetAP1 enzymes are further classified into types Ia, Ib, Ic, and Id. Types Ib, Id, and II MetAPs are expressed in eukaryotes, while types Ia and Ic are present in prokaryotes [9]. Deletion of the MetAP gene is lethal in *E. coli* and *Salmonella typhimurium* demonstrating its crucial role in bacterial survival, and highlighting its potential as a target for the development of novel antibiotics [10,11]. Additionally, inhibition of various MetAPs may have great potential in the treatment of such pathologies as cancer, rheumatoid arthritis, malaria, and atherosclerosis in humans [12].

It has been reported that diketo acid (DKA) derivatives interact with numerous viral enzymes, *i.e.*, HIV-1 integrase [13], HIV-1 RNase [14], influenza endonuclease [15] and hepatitis C RNA polymerase [16]. It might be due to the coordination of diketo functionality with dinuclear Mn(II) or Mg(II) metal ions present in the active site of these enzymes [17]. Since MetAPs also require divalent metal ions for catalysis, it is believed that diketo acid might play a promising role in the inhibition of MetAPs [18]. Based on this hypothesis, we previously reported amino acid/dipeptidic analogues of β-diketo acids and their activity against bacterial MetAPs. The diketo acid derivatives emerged as potent antibacterial agents acting via inhibition of MetAPs [19]. Recently, we also developed LiHMDS catalyzed protocol for C-N bond formation in one step *via in situ* cyclo-condensation of diketo ester to give novel *N*-substituted 2-carboxy-4-quinolones (Fig. 1) [20]. In this study, we report the further optimization of β-diketo acids as potent MetAP inhibitor as well as antibacterial agents. We also synthesized constrained isoxazole ring as biological isosteric analogue of β-diketo acid to investigate rational structure–activity relationship among these compounds. All the synthesized β-diketo acids and their bioisosteres were evaluated against purified MetAPs from *S. pneumoniae* (*Sp*MetAP1a), *M. tuberculosis* (*Mt*MetAP1c), *E. faecalis* (*Ef*MetAP1a) and human (*Hs*MetAP1b). We observed that some of these derivatives showed improved potency against bacterial MetAPs and displayed considerable antibacterial activity.

2. Results and discussion

2.1. Chemistry

The synthesis of diketo acids and their bioisosteres was accomplished as illustrated in Schemes 1–3. Initially, 1-(5-bromo-2-hydroxyphenyl)ethanone on etherification with chloroacetone in the presence of potassium carbonate followed by cyclisation under thermal condition gave benzofuran ketone (**1a**) in good yield (Scheme 1).

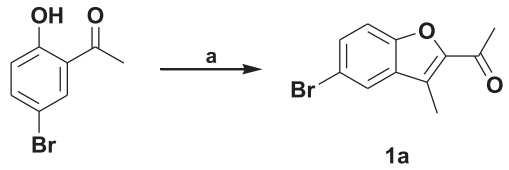

Scheme 1. Synthesis of benzofuran ketone. Reagents and conditions (a) K_2CO_3, DMF, chloroacetone, 80 °C.

The benzofuran ketone (**1a**) and other commercially available aryl methyl ketones (**1b** and **1c**) were subjected to oxalylation by diethyl oxalate in the presence of freshly prepared sodium ethoxide to yield β-diketoesters (**2a-c**) in good yield except diketoester **2a**. It might be due to the inability of sodium ethoxide to abstract α-hydrogen atom of benzofuran ketone (**1a**) with ease due to steric hindrance. Therefore, a much stronger base lithium hexamethyldisilamide (LiHMDS) was employed to effectively execute a sterically hindered Claisen condensation to get the diketoester (**2a**) in excellent yield. Selected β-diketoesters (**2a-b**) were then treated with lithium hydroxide in THF/H_2O mixture (3:1) for 2 h at room temperature to yield corresponding β-diketo acids (**3a-b**) in quantitative yields. Coupling of the β-diketo acids (**3a-b**) with methyl ester of L-alanine using hexafluorophosphate azabenzotriazole tetramethyl uronium (HATU) as coupling reagent and N,N diisopropylethylamine (DIPEA) as a base at room temperature gave L-alanine-methyl ester conjugate of diketo acid (**4a-b**) which was further hydrolyzed by lithium hydroxide to yield corresponding acids (**5a-b**) in quantitative yields (Scheme 2).

In another set of reactions to achieve bioisosteres of β-diketo functionality, the diketo esters (**2a-c**) on reaction with hydroxylamine hydrochloride in absolute ethanol at reflux condition underwent [3+2] cyclocondensation reaction to give isoxazole methyl esters (**6a-c**). Basic hydrolysis of isoxazole methyl esters (**6a-c**) using freshly prepared LiOH solution (2M) in THF/H_2O mixture (3:1) for 4 h gave corresponding acids (**7a-c**) in quantitative yield. L-alanine methyl ester on coupling with isoxazole acids (**7a-c**) in the presence of HATU and DIPEA gave the corresponding isoxazole-alanine methyl ester conjugates (**8a-c**). Alkaline hydrolysis of these isoxazole-alanine methyl ester derivatives (**8a-c**) by lithium

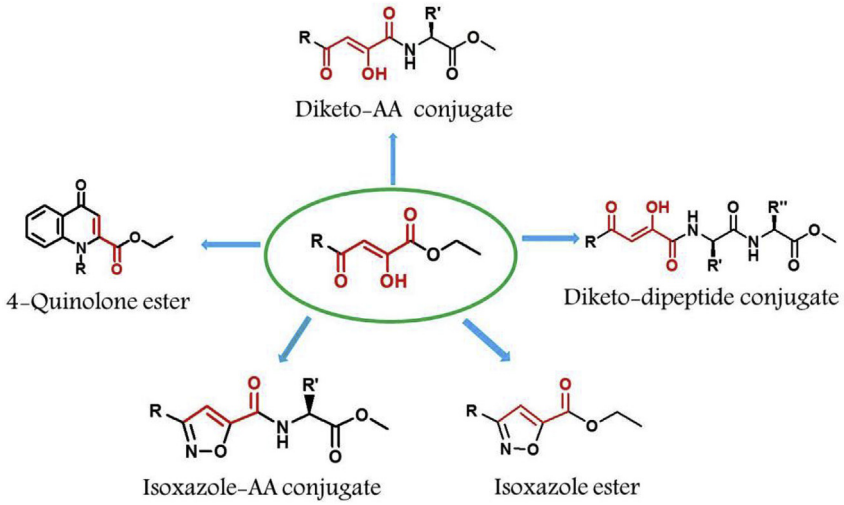

Fig. 1. β-diketo pharmacophore and its bioisosteres.

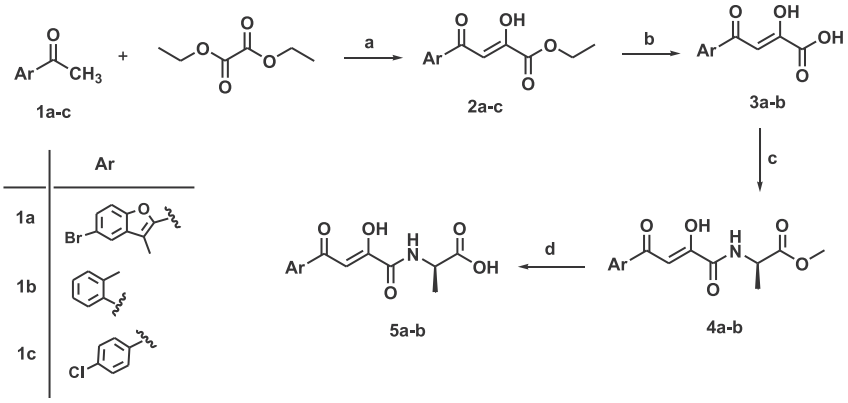

Scheme 2. Synthesis of L-alanine conjugate of diketo acid (**5a-b**). Reagents and conditions (a) LiHMDS (1 M in THF), diethyl oxalate, THF, −50 °C–0 °C, 1 h (for **2a**); Na metal, C_2H_5OH, 0 °C-r.t., 3–4 h (**2b** and **2c**); (b) LiOH.H_2O, THF:H_2O (3:1), r.t., 4 h; (c) HATU/DIPEA, THF, L-alanine methyl ester, r.t., 16 h; (d) LiOH.H_2O, THF:H_2O (3:1), r.t., 4 h.

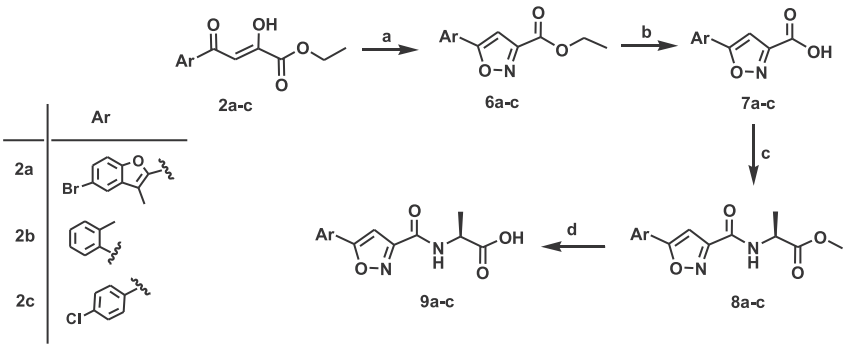

Scheme 3. Synthesis of isoxazole-L-alanine acid conjugates. Reagents and conditions (a) $NH_2OH.HCl$, EtOH, reflux, 4 h; (b) LiOH.H_2O, THF:H_2O (3:1), r.t., 4 h; (c) HATU/DIPEA, THF, L-alanine methyl ester, r.t., 16 h; (d) LiOH.H_2O, THF:H_2O (3:1), r.t., 4 h.

hydroxide afforded corresponding isoxazole-alanine acids (**9a-c**) in quantitative yields (Scheme 3).

The physico-chemical parameters for all the synthesized compounds were evaluated using QikProp version 3.2 from Schrödinger software. All the synthesized compounds were found within the recommended range of important physico-chemical parameters. None of them was found violating the Lipinski's rule of five (Supplementary File).

2.2. X-ray crystallographic analysis

Single X-ray crystal structure analysis of isoxazole acid (**7b**) was carried out to establish the authenticity of the basic structure. X-ray and structure refinement statistics are presented in Table 1. A colorless plate-like specimen of compound **7b** ($C_{11}H_9NO_3$) with approximate dimensions 0.050 × 0.140 × 0.160 mm was used for X-ray diffraction. The compound crystallized in the monoclinic crystal system, using the space group $P2_1/c$, with four molecules in the unit cell. The structure was determined in the monoclinic space group, $P2_1/c$ with four molecules in the asymmetric unit. The XP diagram of compound **7b** with thermal ellipsoids drawn at 30% probability level and with atomic numbering scheme is shown in Fig. 2A. The *o*-tolyl substituent is orientated almost planar compared with the five membered ring (C3-N1-O1-C4-C2), with a deviation angle of 9°. Strong hydrogen bonding interactions involving two adjacent carboxyl groups [O3-H1···O2 2.639(2) Å and 177(3) °] leads to the formation of dimeric units in the solid state of **7b** (Fig. 2B).

Notable is the almost planar structure of this dimeric unit. In the packing diagram, the formation of a linear chain of dimeric units along a-axis involving π ··· π interactions was observed. Shortest distances between these dimeric units are C2···O2 3.226 Å and C2···C10 3.294 Å (Fig. 2C and D). An overlapping mode of these

Table 1
Crystal data and structure refinement details for **7b**.

Identification code	7b
Formula	$C_{11}H_9NO_3$
M_W (g/mol)	203.19
$d_{calcd.}$ (g cm^{-3})	1.446
Crystal size (mm)	0.050 × 0.140 × 0.160
T/K	100(2)
λ (Å)	1.54178
F(000)	424
Crystal System	Monoclinic
Space Group	$P2_1/c$
a(Å)	5.5856(12)
b(Å)	10.373(2)
c(Å)	16.309(3)
α (°)	90
β (°)	98.969(12)
γ (°)	90
V (Å^3)	933.4(3)
Z	4
θ range (°)	5.07–66.68
Collected reflections	12118
Unique reflections; R_{int}	1638 [R_{int} = 0.0767]
μ/mm^{-1}	0.891
$R(F_o)$, [$I > 2\sigma(I)$]	0.0429
R_w (F_o^2) (all data)	0.0595
GoF (F^2)	1.044
Δρ [e Å^{-3}]	0.203/−0.283
CCDC number	**1415262**

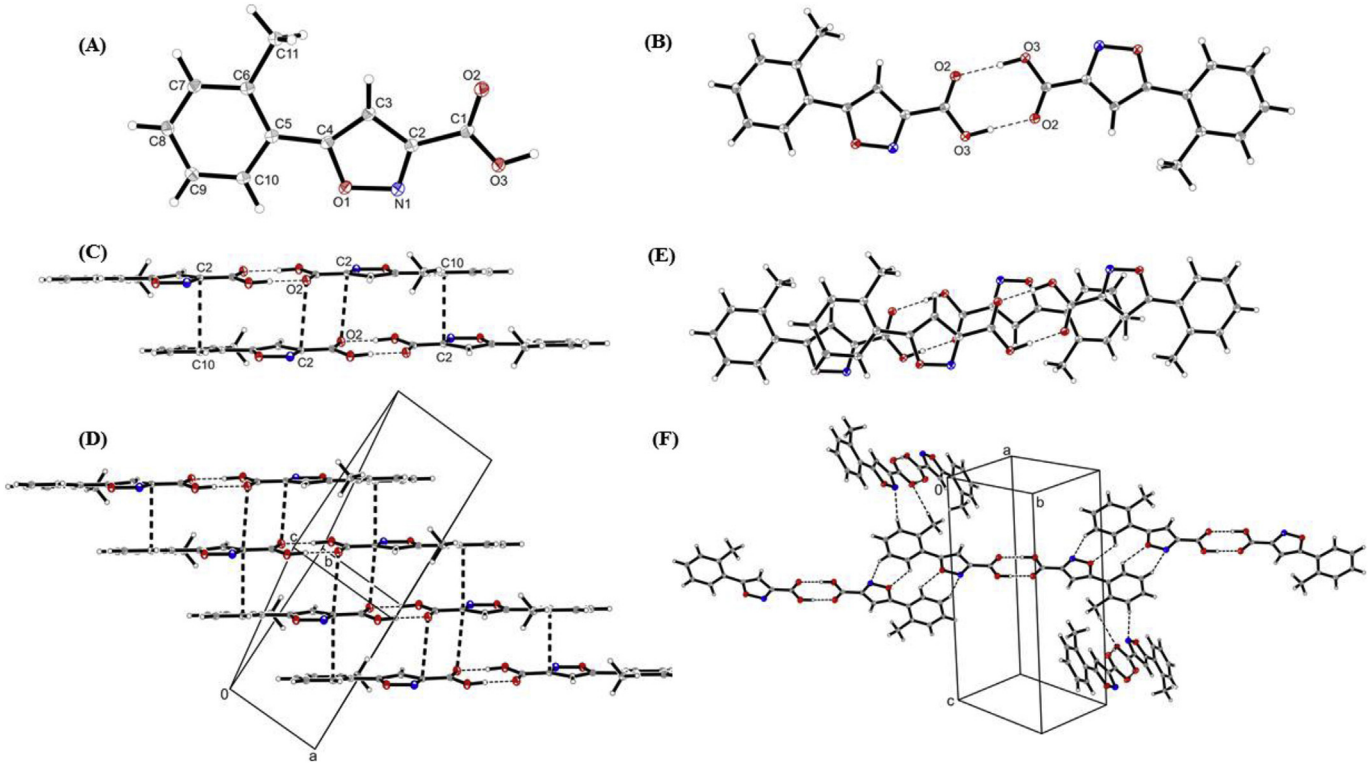

Fig. 2. (A) XP diagram of compound **7b** with atomic numbering scheme (30% probability level of thermal ellipsoids); (B) Dimeric unit formation trough O-H···O hydrogen bonds; (C) Dimer formation trough π ··· π interactions in the solid state of compound **7b**. (D) Excerpt of the packing diagram of compound **7b** presenting the linear chain formation along a-axis; (E) Overlapping mode between two dimeric units in **7b**; (F) Excerpt of the packing diagram of **7b** presenting the C-H···O and C-H···N interactions between the dimeric units.

dimeric units is shown in Fig. 2E. Additionally, non-covalent C-H···O and C-H···N interactions between the *o*-tolyl group and the five membered ring stabilized the crystal structure of **7b** [C9-H9···N1 2.699 Å and 146.5°; C10-H10···O1 2.771 Å and 131.5°; C7-H7···N1 2.834 Å and 171.2°; C11-H11A ··· O3 2.701 Å and 126.1°] (Fig. 2F).

2.3. Biochemical assays: In vitro methionine aminopeptidases (MetAPs) inhibition studies

Mounting evidence suggested that MetAP plays an important role in co- or post-translational modification of proteins thus is crucial for the metabolism and survival of bacterial cells [21]. As we reported earlier, β-diketo esters and their amino acids/dipeptidic analogues emerged as potent antibacterial agents acting via inhibition of bacterial MetAPs. In this work, we designed some diketo esters and their bioisosters and evaluated their effect on inhibition of MetAPs from different origins *viz. H. sapiens, E. feacalis, M. tuberculosis* and *S. pneumoniae*. The inhibitory results (in percentage) and *Ki* values of selected compounds are summarized in Table 2 and Table 3, respectively. Results presented here clearly demonstrated that the transformation of diketoesters into isoxazole resulted in the loss of inhibitory potential against bacterial MetAPs. However, compound **9a** emerged as potent inhibitor of *Hs*MetAP1b among all isoxazole derivatives in the series with 93.39% inhibition (*Ki* = 3.11 μM) indicating selectivity over bacterial enzymes. Among all compounds, benzofuran-containing compounds (**2a**, **3a**, **4a**, and **5a**) displayed the highest inhibition against both human and bacterial MetAPs with better preference to *E. faecalis*. Compound **4a** displayed better selectivity towards *S. pneumoniae* MetAP1a. Surprisingly compound **9a** showed inhibition only against human MetAP1b. Repeated attempts to determine the enzyme inhibitor complexes with all these lead compounds and all enzymes in this study did not succeed which limited our ability to pinpoint the exact molecular basis for this observed selectivity. Based on enzyme inhibition studies, compounds **4a** and **5a** could be considered as potent antibacterial though having some selectivity towards bacterial MetAPs over human enzyme. To better understand the molecular basis, we carried out molecular docking studies.

Table 2
In vitro inhibition study of title compounds against different MetAPs.

Compound	% Inhibition at 100 μM inhibitor concentration			
	HsMetAP1b	*EfMetAP1a*	*MtMetAP1c*	*SpMetAP1a*
2a	85.96 ± 0.85	93.31 ± 0.35	91.63 ± 041	73.05 ± 0.39
2b	61.36 ± 2.88	43.5 ± 2.45	55.83 ± 1.24	50.29 ± 3.02
2c	61.01 ± 2.58	27.34 ± 2.39	70.51 ± 0.54	55.32 ± 1.5
3a	88.15 ± 0.19	91.90 ± 1.04	93.47 ± 0.34	93.4 ± 0.04
3b	52.27 ± 3.44	54.7 ± 3.68	65.69 ± 0.34	62.84 ± 4.6
4a	89.09 ± 0.76	93.86 ± 0.23	99.59 ± 0.02	97.44 ± 0.08
4b	51.88 ± 3.73	59.61 ± 1.37	67.07 ± 0.3	56.96 ± 2.49
5a	87.45 ± 0.66	92.68 ± 0.08	87.65 ± 0.23	98.16 ± 0.07
5b	59.24 ± 2.68	63.23 ± 0.19	47.7 ± 2.62	58.05 ± 1.38
6a	43.57 ± 1.64	21.08 ± 0.27	41.32 ± 0.68	40.59 ± 1.54
6b	48.85 ± 3.78	27.65 ± 1.21	47.09 ± 6.95	41.39 ± 2.35
6c	66.29 ± 3.06	19.43 ± 5.86	47.43 ± 0.5	40.3 ± 0.24
7a	47.26 ± 3.16	40.28 ± 0.43	39.12 ± 2.8	43.24 ± 1.48
7b	48.97 ± 2.96	32.01 ± 1.23	43.72 ± 1.21	42.41 ± 1.47
7c	43.87 ± 5.72	20.01 ± 2.02	58.21 ± 0.98	39.66 ± 2.06
8a	45.08 ± 6.55	18.82 ± 065	36.2 ± 1.12	36.47 ± 1.21
8b	51.09 ± 6.02	24.926 ± 1.16	45.91 ± 0.54	36.95 ± 1.01
8c	43.13 ± 3.91	15.37 ± 3.96	53.16 ± 0.46	43.76 ± 2.62
9a	93.39 ± 0.31	34.62 ± 0.21	33.2 ± 0.62	42.8 ± 2.24
9b	50.22 ± 2.34	43.42 ± 0.67	40.91 ± 1.71	44.65 ± 1.22
9c	47.25 ± 1.58	23.65 ± 2.96	51.66 ± 0.54	43.69 ± 2.05

Table 3
Ki values of potent MetAP inhibitors.

Compound	Ki value (in μM)			
	HsMetAP1b	*EfMetAP1a*	*MtMetAP1c*	*SpMetAP1a*
2a	19.75 ± 1.75	10.79 ± 1.42	18.16 ± 2.17	68.24 ± 4.62
2b	74.31 ± 4.9	ND	36.74 ± 109	98.49 ± 8.94
2c	56.1 ± 2.8	ND	39.5 ± 3.23	62.61 ± 3.1
3a	32.72 ± 2.53	17.67 ± 1.9	26.28 ± 2.3	27.47 ± 1.24
3b	73.8 ± 5.44	62.56 ± 3.96	37.54 ± 1.67	87.5 ± 7.77
4a	22.14 ± 2.2	10.42 ± 1.09	17.59 ± 1.45	8.78 ± 0.89
4b	112.82 ± 6.86	60.35 ± 7.8	32.62 ± 1	51.91 ± 3.17
5a	22.1 ± 1.06	11.89 ± 1.34	9.89 ± 0.66	28.32 ± 1.8
5b	54 ± 2.72	63.96 ± 4.89	ND	59.87 ± 7.55
6b	122.58 ± 7.98	ND	ND	ND
6c	160.43 ± 10.16	ND	152.15 ± 4.9	ND
7b	103.92 ± 6.62	ND	ND	ND
7c	ND	ND	71.81 ± 8.31	ND
8b	136.7 ± 10.35	ND	ND	ND
8c	ND	ND	134.31 ± 9.83	ND
9a	3.11 ± 0.4	ND	ND	ND
9b	86.85 ± 4.7	ND	ND	ND
9c	ND	ND	94.62 ± 6.02	ND

2.4. Docking studies

Glide XP docking of the compounds (**4a** and **5a**) within the active site of different targets show variations in the glide score, model energies and glide energies. The penalty of buried ligands in the cavity makes a very small contribution in all the docking conditions. Among all the energy parameters the largest contribution of the energy comes from electrostatic and van der Waals interactions.

XP docking within the binding site of methionine aminopeptidase Type 1c from *M. tuberculosis* (PDB ID: 1YJ3) indicates the better binding capability of compound **4a** within the binding site compared to **5a**. The model energies of the binding of ligands have been found to be −47.513 and −41.015 kcal/mol respectively. The various non-covalent interactions with the ligands in the binding site of 1YJ3 have been shown in Fig. 3. It has been observed that the residues LYS98, HIS212 and THR203 form N-H···O type hydrogen bonding interactions with both ligands **4a** and **5a**. Hydrophobic and other polar interactions are also similar in both types of ligands. Residues TYR97, TRP255, ILE250, PHE202, MET240 form a hydrophobic enclosure to the ligands. Polar interactions are exhibited by HIS114, HIS212, HIS205 and THR203 residues while ASP201 and GLU238 residues show charge negative interactions.

Docking of ligands within the binding site of *E. faecalis* Methionine aminopeptidase (PDB ID:3TB5) also exhibit the better binding capability of **4a** with Glide score and model energy −5.391 and −58.622 kcal/mol compared to **5a** with Glide score and Glide energy of −5.056 and −46.471 kcal/mol respectively. The contribution of van der Waal and Coulomb energies play significant roles in the binding of ligands. Fig. 3 depicts the interactions of the ligands within the binding site. It can be deduced that several hydrogen bonding and other noncovalent interactions stabilize the compounds within the binding site of 3TB5. N-H···O type hydrogen bonding interactions involves residues GLU201, GLN57, and VAL166. GLU201 also exhibits classical strong O-H.O hydrogen bond formation in the case of binding with **4a**. π-π stacking interactions are displayed by a PHE165 residue with the aromatic moiety of the ligands. Hydrophobic interactions are shown within the binding site by residues TRP218, PHE165, VAL166, CYS96, TYR60, ILE174, and MET178. Residues HIS168, HIS77, GLN57, HIS175, THR199, and GLN230 display polar interactions whereas residues ASP164, ASP94, GLU232, ASP105 and GLU201 exhibit electrostatic interactions.

The Glide score and model energies of the **4a** and **5a** as obtained through extra precision docking within binding site of methionine aminopeptidase from *S. pneumoniae* (PDB ID: 4KM3) were found to be −4.620 and −51.377 kcal/mol; −4.579 and −41.922 kcal/mol respectively. The non-covalent interactions are exhibited in Fig. 3. Residues HIS199, VAL197 and ASP195 form N-H···O hydrogen bonding interactions with both the ligands. Interestingly, His252 residue exhibit C-H … π weak hydrogen bonding interaction in the case of both ligands. Additionally, aromatic π-π interactions are also shown in the best docking pose of **5a** involving TRP250 and an aromatic moiety of the compound. The hydrophobic enclosure is

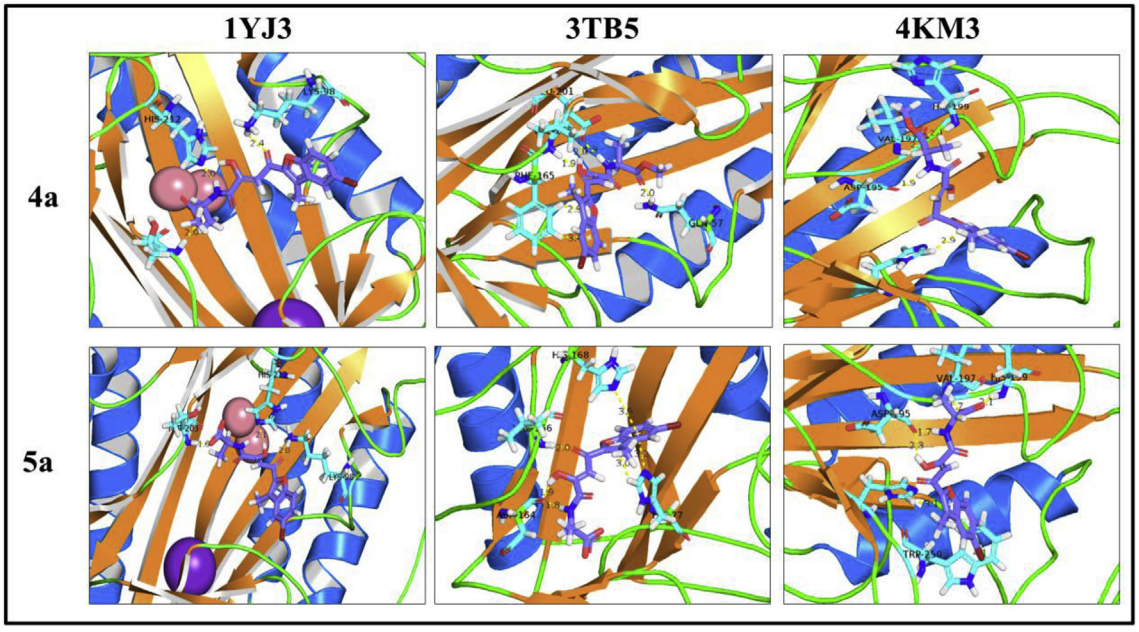

Fig. 3. Docking studies of compounds **4a** and **5a** with MetAPs from *M. tuberculosis* (PDB ID: IYJ3), *E. faecalis* (PDB ID: 3TB5) and *S. pneumoniae* (PDB ID:4KM3) showing their interaction with key residues.

Table 4
In vitro antibacterial activity of diketo acids and their bioisosteres.

Compounds	Minimum Inhibitory Concentration (μg/mL)					
	P. aeruginosa	*S. typhimurium*	*S. pneumoniae*	*E. faecalis*	*K. pneumoniae*	*E. coli*
2a	1000	1000	250	250	500	250
2b	1000	1000	250	250	1000	250
2c	500	500	500	250	>1000	500
3a	125	500	62.5	62.5	1000	1000
3b	1000	1000	500	500	1000	250
4a	125	500	62.5	31.25	500	62.5
4b	1000	1000	125	500	1000	1000
5a	250	500	62.5	125	500	62.5
5b	1000	1000	500	500	1000	1000
6c	500	>1000	1000	500	1000	500
9a	1000	500	250	125	>1000	500
CIP	0.25	0.0156	0.312	0.0625	0.25	0.125

formed by the residues PRO203, ALA63, TRP250, LEU196, VAL197, and TYR214. HIS252, THR244, and HIS199 are involved in the polar interactions. ASP195 also exhibit electrostatic interactions within the binding site.

2.5. In vitro antibacterial activity

Eleven compounds were selected on the basis of MetAP inhibition studies for further evaluation of their antibacterial potential against *P. aeruginosa*, *S. typhimurium*, *S. pneumoniae*, *E. faecalis*, *K. pneumonia*e and *E. coli*. The results in terms of minimum inhibitory concentration (MIC) are presented in Table 4. The results showed an irregular pattern in the antibacterial activity of the compounds. The benzofuran based diketo ester (**2a**) showed a moderate inhibitory effect against Gram-positive *S. pneumoniae* and *E. faecalis* and Gram-negative *E. coli* with MIC value of 250 μg/mL, although its activity against *P. aeruginosa* and *S. typhimurium* was very poor. The corresponding acid, **3a** showed better activity as it was found active against four bacterial strains *viz. P. aeruginosa, S. typhimurium, S. pneumoniae* and *E. faecalis* with MIC values of 62.5–500 μg/mL. The 2-methylphenyl diketo ester (**2b**) and its acid **3b** exhibited moderate effect on *S. pneumoniae*, *E. faecalis* and *E. coli* with MIC ranging from 250 to 500 μg/mL. Similarly, L-alanine methyl ester conjugate of 2-methylphenyl based diketo ester **4b** and its corresponding acid, **5b** were found more active against Gram-positive bacteria *S. pneumoniae* and *E. faecalis* with good to moderate antibacterial activity (MIC ranges between 125 and 500 μg/mL) while no significant inhibition was observed in the case of Gram-negative bacterial strains. *p*-Chlorophenyl diketo acid, **2c** and benzofuran isoxazole based alanine derivative, **9a** exhibited good to moderate inhibition ranging from 125 to 500 μg/mL against all the tested strains except *K. pneumoniae*. Benzofuran-L-alanine methyl ester conjugate (**4a**) and its corresponding acid, (**5a**) emerged as potent inhibitors among these selected synthesized derivatives as they showed better inhibitory activity against all the bacterial strains used in the study. Both these compounds exhibited equal potency with MIC values of 500, 500, 62.5 and 62.5 μg/mL against *S. typhimurium, K. pneumoniae, S. pneumoniae* and *E. coli*, respectively. However, compound **4a** was found to be a better inhibitor than compound **5a** against *P. aeruginosa* and *E. faecalis* in terms of MIC values.

Based on the results obtained on sensitive bacterial strains, compounds **4a** and **5a** were selected for further assessment of their antibacterial activity on eight multidrug resistant *E. coli* strains. It was observed that compound **5a** at a concentration of 512 μg/mL exhibited almost 100% inhibition of *E. coli* MRA11, MRC17, MRC24, MRAE32, and MROB11 strains while at the same concentration compound **4a** caused only 65%, 60%, 76%, 88% and 87% inhibition of the respective strains. Therefore, compound **5a** was found to be more effective than compound **4a** against MDR *E. coli* strains. Even at a concentration of 1024 μg/mL, compound **5a** exhibited more efficacy than compound **4a** and showed more than 95% inhibition of *E. coli* MRAE26 and MRAE33 strains while compound **4a** was able to inhibit these strains only by 54% and 50%, respectively. However, at a concentration of 1024 μg/mL both these compounds were found to be almost equally potent against *E. coli* MRAE44 strain (Fig. 4).

These compounds were further evaluated for their *in vitro* synergistic effect in combination with ciprofloxacin against *E. coli* MRA11, MRC17 and MRAE33 strains. The results showed that the antibacterial efficacy of these compounds against the selected strains MRA11 and MRC17 was not affected in combination with ciprofloxacin while a minor increase in activity was observed against MRAE33. The fractional inhibitory concentration index (FICI) values of compounds **4a** and **5a** suggested that these compounds showed no significant synergy in combination with ciprofloxacin against any of the tested strains (Tables 5 and 6).

2.6. Cytotoxicity assessment of lead inhibitors by MTT assay

Cytotoxicity of selected compounds **4a** and **5a** was determined by cell proliferation assay (MTT) on Chinese hamster ovary (CHO) cell line. The study revealed that compounds **4a** and **5a** were found to be non-toxic at a concentration of 50 μg/mL to CHO cells. However, on increasing the concentration of compounds to 100 μg/mL, compound **4a** exhibited more toxicity compared to compound **5a** on CHO cells with only 50% cell viability while later displayed more than 70% cell viability. The cell viability was further decreased on increasing the concentration of these compounds to 300 μg/mL indicated toxic nature of these compounds at high concentration. Compound **5a** can be considered non-toxic at its MIC values thus selected for further biological evaluation (Fig. 5).

2.7. Growth kinetic studies

Based on the MetAP inhibition as well as the antibacterial effect on sensitive/resistant bacterial strains, compound **5a** was evaluated for its effect on the growth of *P. aeruginosa, E. coli, S. pneumoniae* and *E. faecalis* bacterial strains. The results showed that **5a** exerted significant effect on the growth pattern of these strains and completely inhibited the growth of *S. pneumoniae* and *E. faecalis* even at sub-MIC values with a continuous lag-phase of 24 h. Furthermore, at MIC and 2MIC values no growth was observed in case of *P. aeruginosa* and *E. coli* even after 24 h of incubation. However, at sub-MIC concentration very negligible growth of *E. coli* was observed after 22 h while significant growth of *P.aeruginosa*

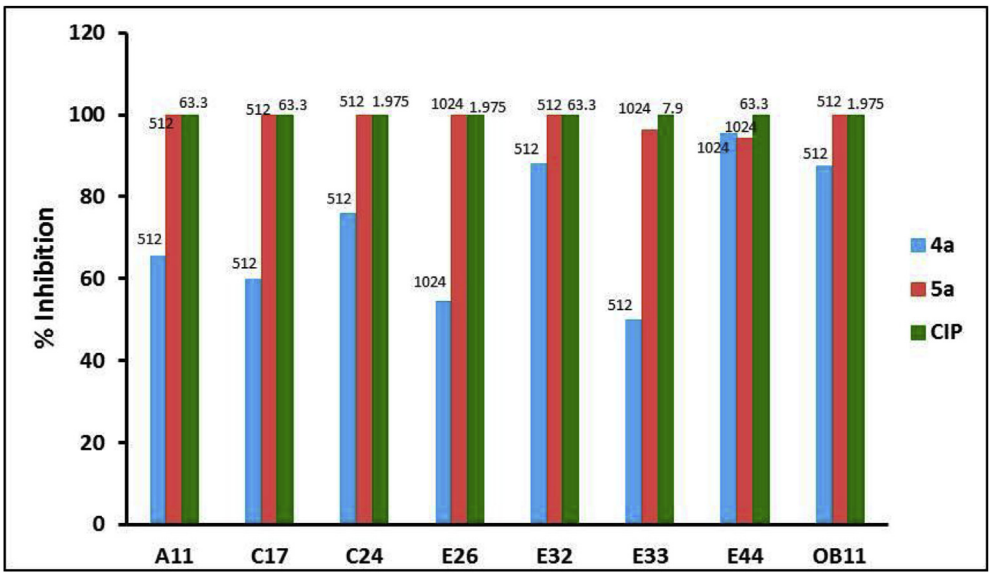

Fig. 4. *In vitro* antibacterial activity of **4a, 5a** and **ciprofloxacin** (μg/mL) against multidrug-resistant *E. coli* strains: MRA11, MRC17, MRC24, MRAE26, MRAE32, MRAE33, MRAE44 and MROB11. The numbers written above the respective columns corresponds to the concentrations of **4a**, **5a** and **CIP** at which maximum inhibition was observed, respectively.

Table 5
In vitro synergistic antibacterial activity of **4a**.

MDR *E. coli* strains	MIC alone (μg/mL)		MIC in combination (μg/mL)		FICI*	Mode of interaction
	4a	CIP	4a	CIP		
MRA11	1024	128	1024	128	2.0	Indifferent
MRC17	1024	128	1024	64	1.5	Indifferent
MRAE33	1024	2	16	2	1.0156	Indifferent

Table 6
In vitro synergistic antibacterial activity of **5a**.

Multidrug resistant *E. coli* strains	MIC alone (μg/mL)		MIC in combination (μg/mL)		FICI*	Mode of interaction
	5a	CIP	5a	CIP		
MRA11	512	128	512	16	1.125	Indifferent
MRC17	512	128	512	64	1.5	Indifferent
MRAE33	1024	2	16	2	1.0156	Indifferent

was observed after 10 h. Therefore, it can be concluded that **5a** is bacteriostatic in nature and effectively arrests the bacterial growth (Fig. 6).

2.8. Assessment of biofilm formation

To see the effect of lead inhibitor (**5a**) on biofilm formation, XTT assay was also performed on *P. aeruginosa, E. coli, K. pneumoniae* and *E. faecalis* strains. Compound **5a** exhibited significant anti-biofilm activity on *E. coli* and *P. aeruginosa* with IC_{50} values of 0.404 and 1.69 μg/mL, respectively. However, this compound showed moderate efficacy on *K. pneumoniae* and *E. faecalis* with IC_{50} values of 113.21 and 1243.08 μg/mL, respectively (Table 7).

SEM analysis was also performed to visualize the effect of **5a** on biofilm formation using *E. coli* strain. Significant inhibition of biofilm development was observed in *E. coli* on treatment with 2MIC concentration of compound **5a**. Clustering of cells which signifies the formation of biofilm was observed in untreated samples while scattered cells with poor cell density were observed in treated cells. So, it can be concluded that the **5a** may have the potential to be an anti-biofilm agent as well as an antibacterial agent (Fig. 7).

2.9. Transmission electron microscopic (TEM) analysis

Structural changes induced by **5a** on *E. coli* and *S. pneumoniae* were characterized using TEM micrographs. The control cells and cells treated with MIC value of **5a** were used for TEM analysis. The untreated cells were observed with normal cell morphology with intact cell membrane and uniform cell density while treated cells showed significant cell damage with several deformations. Distorted cell membrane with leakage of cell cytoplasm was observed in **5a** treated cell micrographs. These results confirmed the cell damaging effect of **5a** on both bacterial strains. (Fig. 8).

2.10. In vivo toxicity evaluation of 5a on Galleria mellonella larvae

It has been reported previously that *G. mellonella* larvae may be utilized as an *in vivo* model for the assessment of toxicity of novel

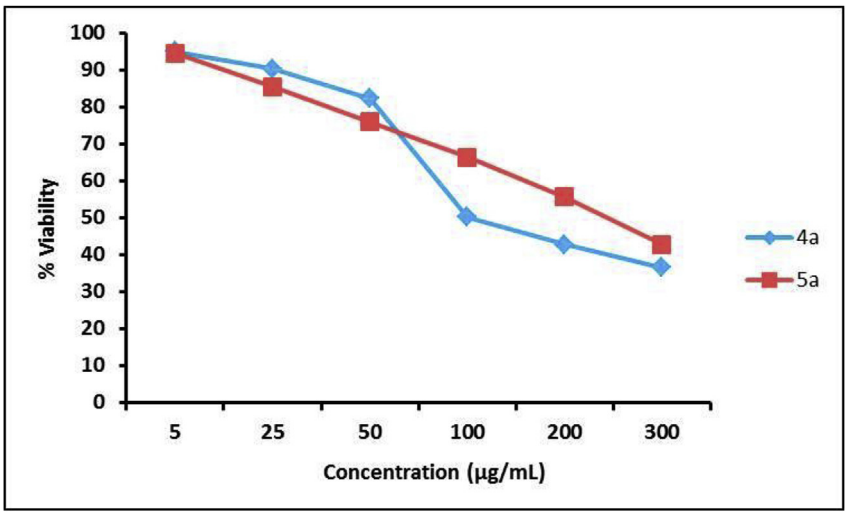

Fig. 5. Cytotoxicity of compounds determined by MTT assay on CHO cell line.

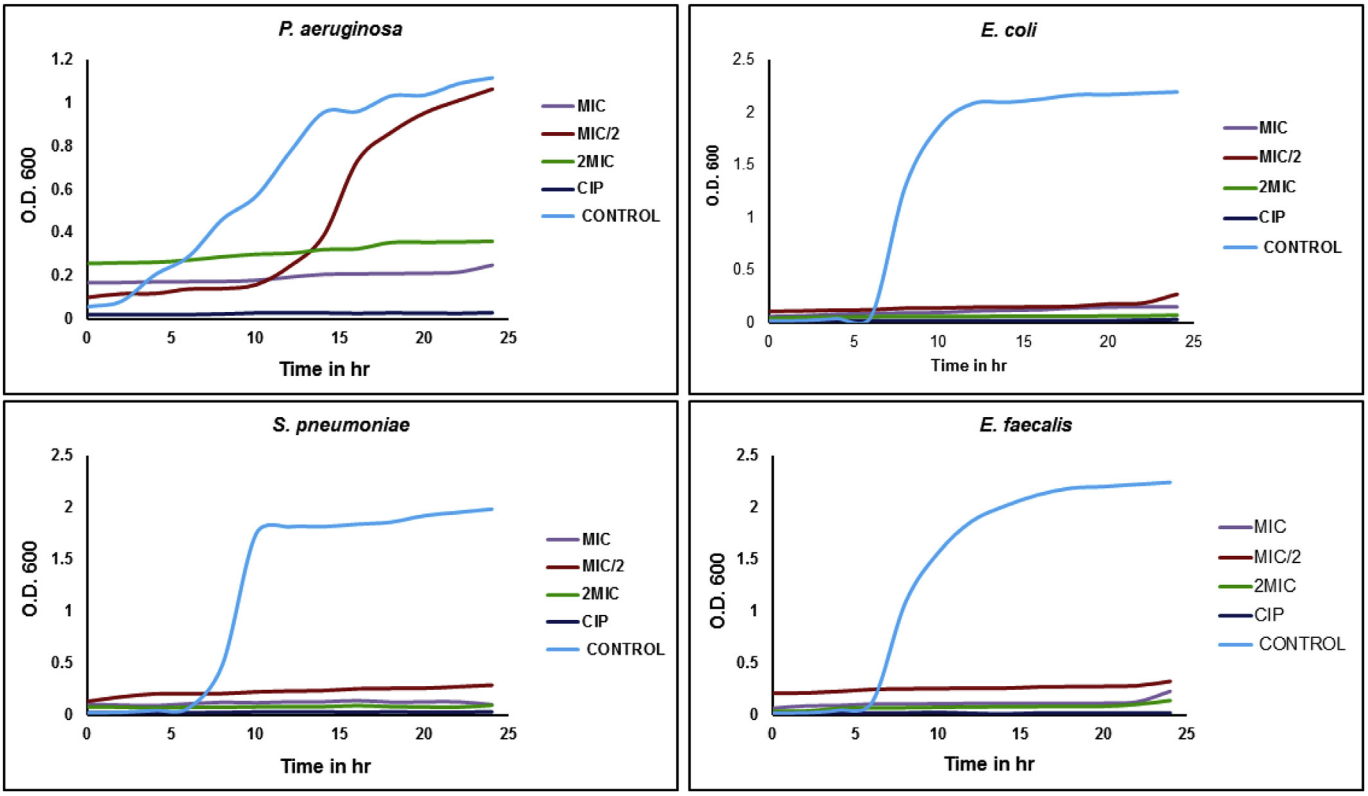

Fig. 6. The effect of different concentrations of compound **5a** on the growth kinetic studies.

antimicrobial agents due to remarkable similarities between the innate immune responses of insects and mammals. Therefore, *G. mellonella* larvae were chosen to determine the *in vivo* toxicity of the lead compound. The results clearly indicated the non-toxic behavior of the compound **5a** up to the concentration of 2.5 mg/mL. Moreover, the hemocyte (immune cell) density of the larvae was not affected at the same concentration indicating the lack of an immune response (Fig. 9).

Table 7
Anti-biofilm activity of compound **5a**; IC_{50} values (µg/mL).

Strain	IC_{50} (µg/mL)
P. aeruginosa	1.69 ± 0.084
E. coli	0.404 ± 0.02
K. pneumoniae	113.21 ± 5.66
E. faecalis	1243.08 ± 62.15

Overall, the study reveals that compound **5a** which is β-diketo acid-alanine conjugate derived from benzofuran ketone conjugated with L-alanine methyl acid was evolved as potent antibacterial agent validated by biochemical and other pharmacological assays. As the metal chelating property of β-diketo functionality disrupt the biological function of MetAPs, compound **5a** significantly

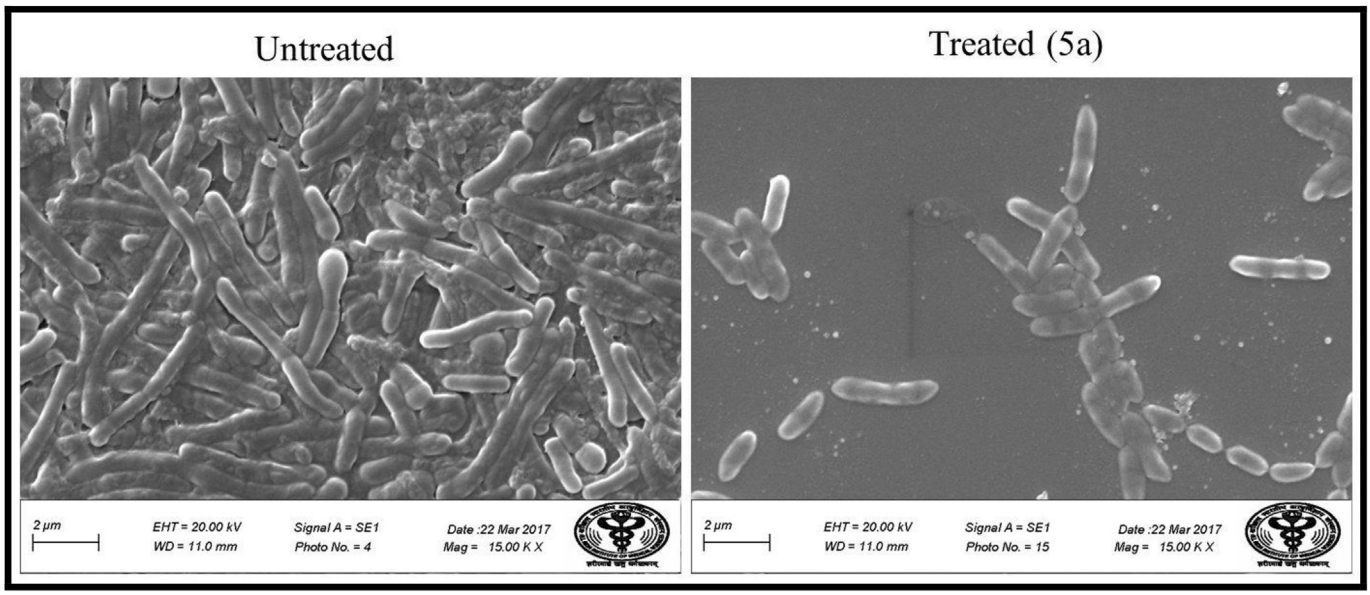

Fig. 7. Scanning electron microscopy of biofilm: Untreated and treated with 2MIC concentration of compound **5a**.

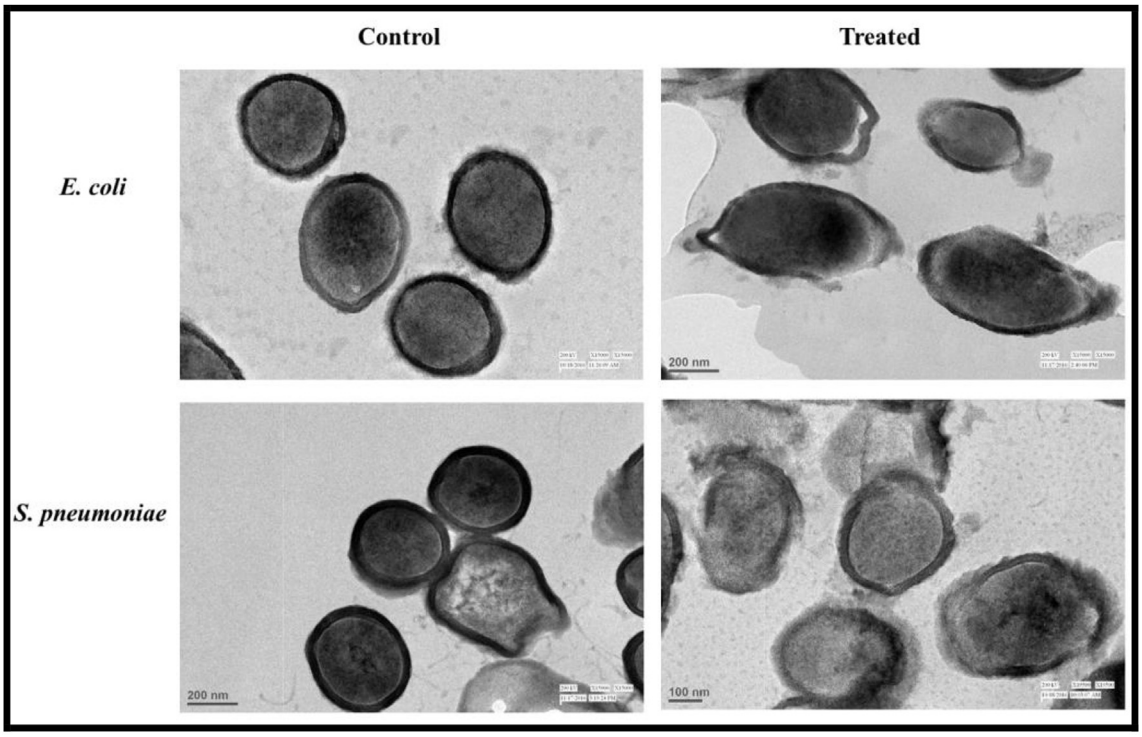

Fig. 8. TEM images showing cellular alteration in *E. coli* and *S. pneumoniae* treated with MIC concentration of **5a**.

inhibited the activity of bacterial MetAPs. Conversion of diketo moiety into a constrained isoxazole ring led to decrease in MetAP inhibition potential, which further confirms diketo moiety is endowed with metal chelating property and essential for MetAP inhibition. Moreover, the selectivity of compounds towards various MetAPs was also determined. Repeated attempts to determine the enzyme-inhibitor complexes with the lead compound and all enzymes in this study did not succeed which limited our ability to pinpoint the exact molecular basis for this observed selectivity. The study on multidrug resistance (MDR) strains of *E. coli* as well as cytotoxicity data support the candidature of compound **5a** as the lead inhibitor. Further pharmacological experiments were in favour of preliminary biological results which indicate **5a** as potent antibacterial agent.

3. Conclusion

To summarize, a series of diketo esters and their bioisosteres were designed as methionine aminopeptidase (MetAP) inhibitors and evaluated for their antibacterial potential against a panel of

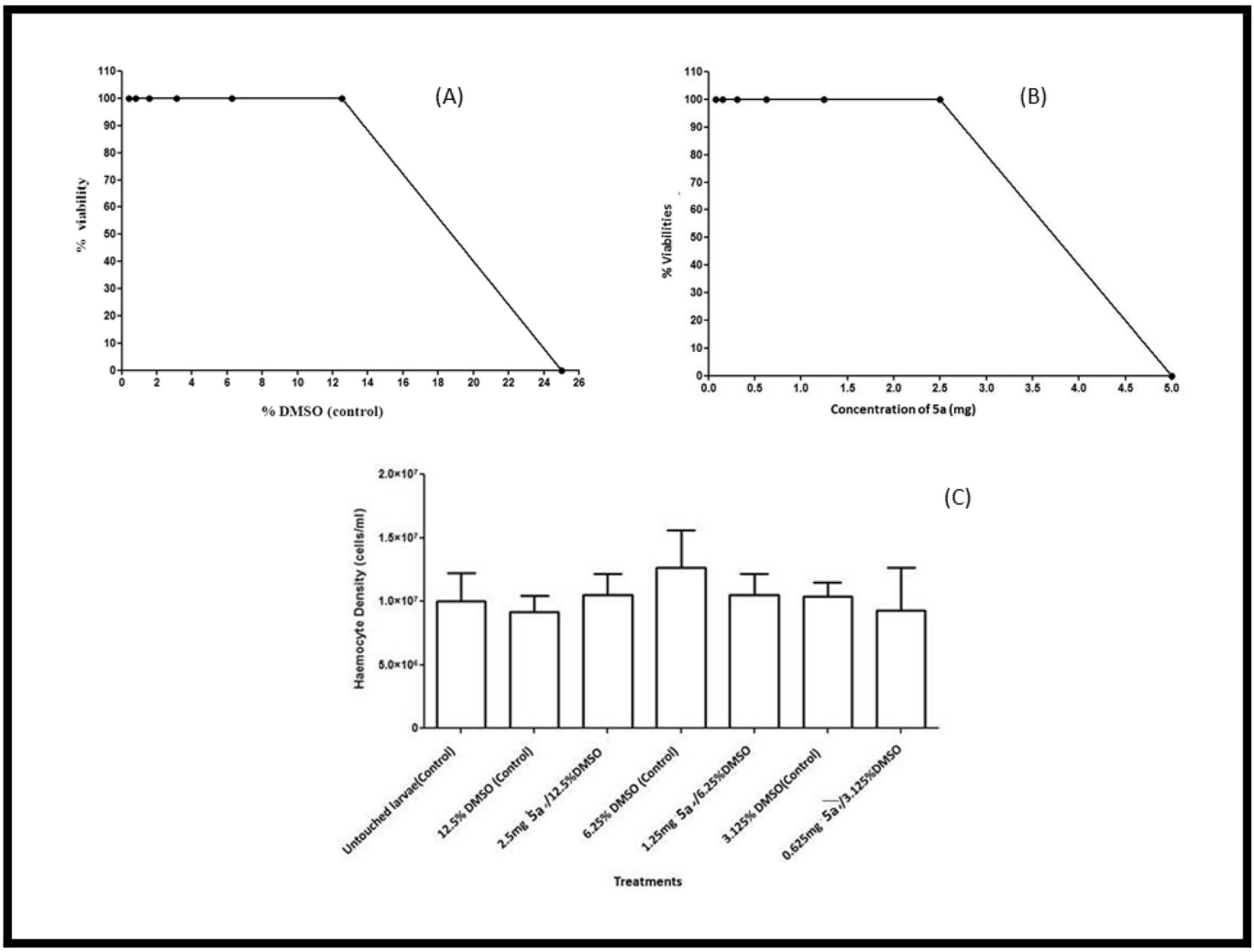

Fig. 9. Effect of (A) DMSO and (B) **5a** on the percentage viability of *G. mellonella*; (C) Haemocyte densities of larvae.

Gram-negative and Gram-positive bacteria. Among all, compounds **4a** and **5a** exhibited more than 85% inhibition against *Sp*MetAP, *Mt*MetAP, *Ef*MetAP and *Hs*MetAP, at 100 μM. Moreover, these compounds displayed considerable potency against several Gram-positive as well as Gram-negative bacterial strains. The considerable efficacy and non-toxic nature of compound **5a** encouraged us to investigate its pharmacological potential. Compound **5a** also inhibited the growth of various bacterial strains at different concentrations as signified by growth kinetics study. Compound **5a** also inhibited the formation of biofilm in *E. coli* as seen in SEM micrographs. TEM micrographs showed that compound **5a** exhibited significant membrane disruption and cell-wall damage in bacterial cells (*S. pneumoniae* and *E. coli*). Besides, this compound did not cause alteration in hemocyte density in *G. mellonella* larvae and was non-toxic up to a concentration of 2.5 mg/mL. Furthermore, efforts in modifying these and other lead structures with the aim of improving potency as well as specificity are in progress.

4. Experimental section

4.1. Chemical synthesis

All the reagents and solvents (analytical grade) were procured from Sigma-Aldrich, USA. Reactions were monitored by thin-layer chromatographic analysis on pre-coated Merck silica gel 60 F_{254} TLC aluminum sheets. Infrared spectra were recorded on Agilent Cary 630 FT-IR spectrometer; wave numbers are given in cm^{-1}. ^1H and ^{13}C NMR spectra were obtained on BrukerSpectrospin DPX-300 spectrometer at 300 MHz and 75 MHz, respectively or a Bruker-Avance II 400 spectrometer at 400 MHz. ^1H and ^{13}C NMR chemical shifts (δ) values are reported in parts per million (ppm) relative to residual solvent $CDCl_3$, δ 7.26 and 77.16; DMSO-d_6, δ 2.54 and 39.5, respectively with tetramethylsilane (TMS) as an internal standard. Splitting patterns are designated as follows: s (singlet), d (doublet), t (triplet), q (quartet), m (multiplet) or brs (broad) and coupling constants (J) are expressed in Hertz (Hz). Mass spectra were recorded on Agilent RRLC MS 6320 ion trap spectrometer fitted with electrospray ionization (ESI) interface or Waters ZQ Single Quadrupole Detector (SQD) electron spray ionization mass spectrometer. Ultra performance liquid chromatography was performed on API 2000 triple quadrupole detector (TQD) mass spectrometer (UPLC-MS/MS). Melting points were recorded on a digital Buchi melting point apparatus (M-560) and are uncorrected. Purification of the compounds was carried out by flash column chromatography (silica gel, 230–400 mesh size, Merck, Germany) with the indicated solvent.

4.1.1. Synthesis of benzofuran ketone (***1a***)

To the stirred solution of 1-(5-bromo-2-hydroxyphenyl)

ethanone (5.0 g, 23.25 mmol, 1.0 eq) in DMF (2 mL/mmol) was added K_2CO_3 (9.62 g, 69.76 mmol, 3.0 eq) and the mixture was stirred at room temperature for 30 min. Chloroacetone (2.0 eq) was added and the reaction mixture was refluxed at 80 °C for 4 h. After completion of reaction (monitored by TLC), the reaction mixture was cooled, quenched with water and extracted with diethyl ether. The combined organic layers were washed with brine solution, dried over anhydrous Na_2SO_4, filtered and concentrated under *vacuo*. The crude was purified by column chromatography over 230–400 silica gel eluting with 10% ethyl acetate in hexane to afford off white benzofuran ketone [22].

*4.1.1.1. 1-(5-bromo-3-methylbenzofuran-2-yl) ethanone (**1a**).* Off white solid, yield: 66%, mp 115–117 °C, R_f (hexane: ethyl acetate = 7:3): 0.83, ^{1}H NMR (400 MHz, DMSO-d_6) (δ, ppm): 8.09 (s, 1H, Ar-*H*), 7.68 (s, 2H, Ar-*H*), 2.56 (s, 3H, C*H*$_3$), 2.53 (s, 3H, C*H*$_3$). ^{13}C NMR (75 MHz, $CDCl_3$) (δ, ppm): 191.16, 152.57, 148.96, 131.29, 131.06, 124.20, 123.23, 116.32, 113.68, 27.83, 9.37. LC-MS (*m/z*): 253.08 $[M + H]^+$. IR (neat): 1687, 1577, 1361, 1272 cm^{-1}.

4.1.2. General synthesis of diketo esters (2a-c)

A solution of ketone (**1a-c**) (1.0 eq) in anhydrous THF (5 mL/mmol) was added dropwise to a solution of LiHMDS (1 M solution in THF) (2.5 eq) at −50 °C and the reaction mixture was stirred at the same temperature for 30 min. A solution of diethyl oxalate (1.1 eq) in THF (1 mL/mmol) was added and the reaction mixture was stirred at 0 °C for 1 h. After completion of reaction, the reaction mixture was quenched by adding water, acidified with 1 N HCl up to pH 2–3 and extracted with ethyl acetate (3 × 100 mL). The combined organic layers were washed with brine, dried over anhyd. Na_2SO_4, filtered and concentrated under *vacuo*. The crude was purified by column chromatography over 230–400 silica gel eluted with 10% ethyl acetate in hexane to afford diketo esters [23].

*4.1.2.1. (Z)-ethyl 4-(5-bromo-3-methylbenzofuran-2-yl)-2-hydroxy-4-oxobut-2-enoate (**2a**).* Light yellow solid, mp 169–171 °C, yield: 59%, R_f (hexane: ethyl acetate = 7:3): 0.17, ^{1}H NMR (400 MHz, DMSO-d_6) (δ, ppm): 8.14 (s, 1H, Ar-*H*), 7.73 (s, 2H, Ar-*H*, =C*H*), 6.98 (s, 1H, Ar-*H*), 4.33 (q, 2H, *J* = 7.05, C*H*$_2$), 2.62 (s, 3H, C*H*$_3$), 1.31 (t, 3H, *J* = 7.1, C*H*$_2$). ^{13}C NMR (75 MHz, $CDCl_3$) (δ, ppm): 183.55, 167.74, 161.99, 153.35, 146.76, 131.68, 131.41, 126.07, 124.11, 116.69, 113.70, 99.85, 62.68, 14.12, 9.61. x LC-MS (*m/z*): 352.9 $[M+H]^+$. IR (neat): 1726, 1570, 1145 cm^{-1}.

4.1.2.2. (Z)-ethyl 2-hydroxy-4-oxo-4-(2-methylphenyl)-but-2-enoate (2b). Yellow oil, yield: 65%, R_f (hexane: ethyl acetate = 7:3): 0.66, ^{1}H NMR (300 MHz, DMSO-d_6) (δ, ppm): 12.79 (brs, 1H, O*H*), 7.62 (d, 1H, *J* = 7.6 Hz, Ar-*H*), 7.41 (t, 1H, *J* = 7.0 Hz, Ar-*H*), 7.30–7.25 (m, 2H, Ar-*H*), 6.82 (s, 1H, Ar-*H*), 4.38 (q, 2H, *J* = 7.2, C*H*$_2$), 2.54 (s, 3H, CH_3), 1.39 (t, 3H, *J* = 7.2 Hz, C*H*$_3$). LC-MS: *m/z* $[M + H]^+$ 235.5. IR (neat): 2985, 1734, 1611, 1261, 1019 cm^{-1}.

*4.1.2.3. (Z)-ethyl 4-(4-chlorophenyl)-2-hydroxy-4-oxobut-2-enoate (**2c**).* Yellow solid, mp 189–191 °C, yield: 63%, R_f (hexane: ethyl acetate = 7:3): 0.66, ^{1}H NMR (300 MHz, DMSO-d_6) (δ, ppm): 14.79 (brs, 1H, O*H*), 8.09 (d, 2H, *J* = 7.4 Hz, Ar-*H*), 7.64 (d, 2H, *J* = 7.8 Hz, Ar-*H*), 7.12 (s, 1H, Ar-*H*), 4.32 (q, 2H, *J* = 6.9, C*H*$_2$), 1.31 (t, 3H, *J* = 7.1 Hz, C*H*$_3$). LC-MS (*m/z*): 255.3 $[M+H]^+$. IR (neat): 1734, 1592, 1261 cm^{-1}.

*4.1.3. General synthesis of diketo acids (DKA) (**3a-b**)*

To the stirred solution of diketoester (1.0 eq) in the mixture of THF and water (3:1, 5 mL/mmol) was added lithium hydroxide (2.2 eq) and the reaction mixture was stirred at room temperature for 4 h. The reaction mixture was concentrated under *vacuo*, water was added, acidified with 1 N HCl up to pH-2~3 and extracted with ethyl acetate. The combined organic layers were washed with brine solution, dried over anhyd. Na_2SO_4, filtered and concentrated under *vacuo* to afford pure diketo acid [24].

*4.1.3.1. (Z)-4-(5-bromo-3-methylbenzofuran-2-yl)-2-hydroxy-4-oxobut-2-enoic acid (**3a**).* Yellow solid, mp 189–191 °C (decomposed), yield: 86%, R_f (hexane: ethyl acetate = 7:3): 0.0, ^{1}H NMR (400 MHz, DMSO-d_6) (δ, ppm): 8.11 (s, 1H, Ar-*H*), 7.70 (s, 2H, Ar-*H*, =C*H*), 6.87 (s, 1H, Ar-*H*), 2.60 (s, 3H, C*H*$_3$). ^{13}C NMR (75 MHz, $CDCl_3$) (δ, ppm): 183.26, 167.94, 163.18, 152.79, 146.41, 131.07, 130.93, 125.25, 123.57, 116.09, 113.24, 99.41, 9.10. LC-MS (*m/z*): 323.2 $[M-2H]^-$. IR (neat): 1741, 1719, 1577, 1249, 1089 cm^{-1}.

*4.1.3.2. (Z)-2-hydroxy-4-oxo-4-(2-methylphenyl)-but-2-enoic acid (**3b**).* Yellow solid, mp 108–110 °C, yield: 84%, R_f (hexane: ethyl acetate = 7:3): 0.0, ^{1}H NMR (300 MHz, $CDCl_3$) (δ, ppm): 7.66 (d, 1H, *J* = 7.5 Hz, Ar-*H*), 7.44 (d, 1H, *J* = 6.9 Hz, Ar-*H*), 7.31–7.26 (m, 1H, Ar-*H*), 6.93 (s, 1H, =C*H*), 6.09 (s, 1H, O*H*), 2.57 (s, 3H, C*H*$_3$). LC-MS (*m/z*): 206.9 $[M+H]^+$. IR (neat): 1711, 1633, 1275, 1037 cm^{-1}.

*4.1.4. General synthesis of coupling of diketo acid with L-alanine methyl ester (L-Ala-OCH$_3$) (**4a-b**)*

To the stirred solution of diketo acid (1.0 eq) in dry THF (5 mL/mmol) was added *N,N*-diisopropylethylamine (DIPEA) (2 eq) and HATU (1.5 eq) and the reaction mixture was stirred at room temperature for 20 min. *L*-alanine methyl ester (1.1 eq) was added and the reaction mixture was stirred at room temperature for 16 h. After completion, the reaction mixture was quenched with water and extracted with ethyl acetate. The combined organic layers were washed with brine solution, dried over anhyd. Na_2SO_4, filtered and concentrated under *vacuo*. The crude obtained was purified with column chromatography eluted with 20% ethyl acetate in hexane to afford the title compounds [25].

*4.1.4.1. (R,Z)-methyl 2-(4-(5-bromo-3-methylbenzofuran-2-yl)-2-hydroxy-4-oxobut-2-enamido)propanoate (**4a**).* Off white solid, mp 163–165 °C, yield: 67%, R_f (hexane: ethyl acetate = 7:3): 0.17, ^{1}H NMR (400 MHz, DMSO-d_6) (δ, ppm): 9.21 (d, 1H, *J* = 7.2 Hz, N*H*), 8.13 (s, 1H, Ar-*H*), 7.74 (s, 2H, Ar-*H*, =C*H*), 6.98 (s, 1H, Ar-*H*), 4.46 (q, 1H, *J* = 6.76 Hz, C*H*), 3.65 (s, 3H, OC*H*$_3$), 2.62 (s, 3H, Ar-C*H*$_3$), 1.39 (d, 3H, *J* = 7.2 Hz, C*H*$_3$). ^{13}C NMR (75 MHz, $CDCl_3$) (δ, ppm): 179.63, 175.49, 172.53, 160.62, 153.51, 146.11, 131.43, 125.46, 124.37, 123.87, 116.58, 113.62, 96.26, 52.67, 48.22, 18.22, 9.58. LC-MS (*m/z*): 411.9 $[M + H]^+$. IR (neat): 3432,1756, 1633, 1208, 1138, 1086 cm^{-1}.

*4.1.4.2. (Z)-methyl 2-(2-hydroxy-4-oxo-4-(2-methylphenyl)-but-2-enamido) propanoate (**4b**).* Yellow oil, yield: 59%, R_f (hexane: ethyl acetate = 7:3): 0.56, ^{1}H NMR (400 MHz, DMSO-d_6) (δ, ppm): 9.19 (d, 1H, *J* = 6.6 Hz, N*H*), 7.68 (d, 1H, *J* = 7.4 Hz, Ar-*H*), 7.49–7.48 (m, 1H, Ar-*H*), 7.37–7.35 (m, 2H, Ar-*H*), 6.72 (s, 1H, =C*H*), 4.47–4.41 (m, 1H, C*H*), 3.64 (s, 3H, OC*H*$_3$), 2.43 (s, 3H, C*H*$_3$), 1.38 (d, 3H, *J* = 7.2 Hz, C*H*$_3$). ^{13}C NMR (75 MHz, $CDCl_3$) (δ, ppm): 162.51, 143.24, 136.12, 134.88, 129.73, 129.29, 128.71, 127.99, 125.98, 121.44, 117.76, 57.61, 31.69, 28.75, 21.42. LC-MS (*m/z*): 292.4 $[M + H]^+$. IR (neat): 3346, 2959, 1745, 1685, 1514, 1454 cm^{-1}.

*4.1.5. General hydrolysis of diketo acid-L-alanine methyl ester (DKA-Ala-OCH$_3$) conjugates (**5a-b**)*

To the stirred solution of DKA-Ala-OCH_3 (1.0 eq) in the mixture of THF and water (3:1, 5 mL/mmol) was added lithium hydroxide (2.2 eq) and the reaction mixture was stirred at room temperature for 4 h. The reaction mixture was concentrated under *vacuo*, water was added, acidified with 1 N HCl up to pH-2~3 and extracted with ethyl acetate (3 × 100 mL). The combined organic layers were washed with brine solution, dried over anhyd. Na_2SO_4, filtered and

concentrated under *vacuo* to afford desired compounds [24].

*4.1.5.1. (R,Z)-2-(4-(5-bromo-3-methylbenzofuran-2-yl)-2-hydroxy-4-oxobut-2-enamido) propanoic acid (**5a**).* Off-white solid, mp 196–198 °C (decomposed), yield: 78%, R_f (hexane: ethyl acetate = 7:3): 0.0, ^{1}H NMR (400 MHz, DMSO-d_6) (δ, ppm): 12.05 (s, 1H, O*H*), 9.01 (d, 1H, *J* = 7.5 Hz, N*H*), 8.12 (s, 1H, Ar-*H*), 7.72 (s, 2H, Ar-*H*, =C*H*), 6.98 (s, 1H, Ar-*H*), 4.39–4.36 (m, 1H, C*H*), 2.62 (s, 3H, Ar-CH_3), 1.39 (d, 3H, *J* = 7.2 Hz, CH_3). ^{13}C NMR (75 MHz, $CDCl_3$) (δ, ppm): 175.32, 173.22, 159.95, 152.47, 145.45, 130.74, 124.84, 123.25, 115.86, 113.02, 95.59, 47.62, 17.38, 8.95. LC-MS (*m/z*): 397.7 $[M + H]^+$. IR (neat): 3335, 1722, 1659, 1536, 1086 cm^{-1}.

*4.1.5.2. (R,Z)-2-(2-hydroxy-4-oxo-4-(2-methylphenyl)-but-2-enamido) propanoic acid (**5b**).* Yellow solid, mp 101–103 °C, yield: 68%, R_f (hexane: ethyl acetate = 7:3): 0.0, ^{1}H NMR (400 MHz, DMSO-d_6) (δ, ppm): 12.76 (brs, 1H, O*H*), 8.98 (d, 1H, *J* = 7.2 Hz, N*H*), 7.68 (d, 1H, *J* = 7.2 Hz, Ar-*H*), 7.49–7.47 (m, 1H, Ar-*H*), 7.37–7.36 (m, 2H, Ar-*H*), 6.72 (s, 1H, =C*H*), 4.40–4.36 (m, 1H, C*H*), 2.41 (s, 3H, CH_3), 1.38 (d, 3H, *J* = 7.2 Hz, CH_3). ^{13}C NMR (75 MHz, $CDCl_3$) (δ, ppm): 192.07, 176.64, 175.37, 161.29, 138.20, 134.73, 132.01, 131.87, 129.19, 126.04, 98.42, 48.15, 21.14, 17.88. LC-MS (*m/z*): 278.3 $[M + H]^+$. IR (neat): 3335, 1741, 1659, 1532, 1197 cm^{-1}.

*4.1.6. General method for synthesis of isoxazole methyl ester (**6a-c**)*

To the stirred solution of diketo ester (1.0 eq) in ethanol (5 mL/mmol) was added hydroxylamine hydrochloride (3 eq) and the reaction mixture was refluxed for 4 h. After completion of the reaction, the reaction mixture was cooled to room temperature. The solid precipitate obtained was filtered over sintered funnel and washed with ethanol. The solid product was dried under *vacuo* to afford isoxazole methyl ester [26].

*4.1.6.1. Ethyl 3-(5-bromo-3-methylbenzofuran-2-yl) isoxazole-5-carboxylate (**6a**).* Creamish solid, mp 170–172 °C, yield: 74%, R_f (hexane: ethyl acetate = 7:3): 0.86, ^{1}H NMR (400 MHz, DMSO-d_6) (δ, ppm): 8.07 (s, 1H, Ar-H), 7.67 (d, 1H, *J* = 8.4 Hz, Ar-*H*), 7.62 (d, 1H, *J* = 8.8 Hz, Ar-*H*), 7.34 (s, 1H, Ar-*H*), 4.42 (q, 2H, *J* = 6.8 Hz, CH_2), 2.53 (s, 3H, CH_3), 1.35 (t, 3H, *J* = 7.0 Hz, CH_3).^{13}C NMR (75 MHz, $CDCl_3$) (δ, ppm): 163.69, 159.60, 156.55, 153.39, 140.58, 131.46, 129.56, 123.16, 117.73, 116.45, 113.06, 101.93, 62.42, 14.15, 8.62. LC-MS (*m/z*): 352.2 $[M + 2H]^+$. IR (neat): 3093, 2985, 1726, 1618, 1443, 1261 cm^{-1}.

*4.1.6.2. Ethyl 3-(2-methylphenyl)-isoxazole-5-carboxylate (**6b**).* Light yellow solid, mp 60–62 °C, yield: 70%, R_f (hexane: ethyl acetate = 7:3): 0.86, ^{1}H NMR (300 MHz, $CDCl_3$) (δ, ppm): 7.74 (d, 1H, *J* = 8.4 Hz, Ar-*H*), 7.41–7.27 (m, 3H, Ar-*H*), 6.84 (s, 1H, Ar-*H*), 4.48 (q, 2H, *J* = 10.6 Hz, CH_2), 2.52 (s, 3H, CH_3), 1.45 (t, 3H, *J* = 7.0 Hz, CH_3). ^{13}C NMR (75 MHz, CDCl3) (d, ppm): 168.54, 162.43, 157.87, 136.4, 130.32, 129.56, 128.65, 127.61, 125.92, 101.23, 60.41, 17.72, 14.59. LC-MS: *m/z* $[M + H]^+$232.4. IR (neat): 2988, 1741, 1432, 1227 cm^{-1}.

*4.1.6.3. Ethyl 3-(4-chlorophenyl) isoxazole-5-carboxylate (**6c**).* White solid, mp 62–64 °C, yield: 74%, R_f (hexane: ethyl acetate = 7:3): 0.83, ^{1}H NMR (400 MHz, DMSO-d_6) (δ, ppm): 8.00 (d, 2H, *J* = 8.4 Hz, Ar-*H*), 7.64 (d, 2H, *J* = 8.4 Hz, Ar-*H*), 7.57 (s, 1H, Ar-*H*), 4.40 (q, 2H, *J* = 7.1 Hz, CH_2), 1.34 (t, 3H, *J* = 7.1 Hz, CH_3). ^{13}C NMR (75 MHz, $CDCl_3$) (δ, ppm): 170.56, 159.85, 157.06, 136.97, 129.50, 127.19, 125.09, 100.24, 62.31, 14.15. LC-MS (*m/z*): 252.23 $[M + H]^+$. IR (neat): 3134, 2988, 1726, 1451 cm^{-1}.

*4.1.7. General method for the hydrolysis of isoxazole methyl ester (**7a-c**)*

To the stirred solution of isoxazole methyl ester (1.0 eq) in the mixture of THF and water (3:1, 5mL/mmol) was added lithium hydroxide (2.2 eq) and the reaction mixture was allowed to stir at room temperature for 4 h. After completion of the reaction, the mixture was concentrated under *vacuo*, added water, acidified with 1 N HCl upto pH-2~3 and extracted with ethyl acetate (3 × 100 mL). The combined organic layers were washed with brine solution, dried over anhydrous Na_2SO_4, filtered and concentrated under *vacuo* to afford isoxazole acid [24].

*4.1.7.1. 3-(5-bromo-3-methylbenzofuran-2-yl) isoxazole-5-carboxylic acid (**7a**).* Creamish solid, mp 185–187 °C, yield: 82%, R_f (hexane: ethyl acetate = 7:3): 0.0, ^{1}H NMR (300 MHz, DMSO-d_6) (δ, ppm): 8.00 (s, 1H, Ar-*H*), 7.59 (q, 2H, *J* = 8.9 Hz, Ar-*H*), 7.19 (s, 1H, Ar-*H*), 2.51 (s, 3H, CH_3).^{13}C NMR (75 MHz, $CDCl_3$) (δ, ppm): 164.29, 159.71, 155.85, 153.87, 141.08, 131.73, 130.86, 123.56, 117.45, 115.95, 114.86, 101.47, 8.72. LC-MS (*m/z*): 276.0 [M -COOH]$^-$. IR (neat): 2880,1715, 1644, 1447 cm^{-1}.

*4.1.7.2. 3-(2-methylphenyl)-isoxazole-5-carboxylic acid (**7b**).* White solid, mp 148–150 °C, yield: 86%, R_f (hexane: ethyl acetate = 7:3): 0.0, ^{1}H NMR (300 MHz, $CDCl_3$) (δ, ppm): 7.76 (d, 1H, *J* = 8.7 Hz, Ar-*H*), 7.43–7.33 (m, 3H, Ar-*H*), 6.91 (s, 1H, Ar-*H*), 5.68 (brs, 1H, O*H*), 2.54 (s, 3H, CH_3). ^{13}C NMR (75 MHz, CDCl3) (d, ppm): 167.84, 161.83, 157.37, 135.76, 131.02, 129.66, 127.95, 127.31, 125.82, 101.54, 17.52. LC-MS (*m/z*): 204.2 $[M + H]^+$. IR (neat): 2955, 2869, 1704, 1264 cm^{-1}.

*4.1.7.3. 3-(4-chlorophenyl) isoxazole-5-carboxylic acid (**7c**).* White solid, mp 201–203 °C, yield: 75%, R_f (hexane: ethyl acetate = 7:3): 0.0, ^{1}H NMR (400 MHz, DMSO-d_6) (δ, ppm): 14.11 (brs, 1H, -COO*H*), 7.98 (d, 2H, *J* = 8.4 Hz, Ar-*H*), 7.64 (d, 2H, *J* = 8.5 Hz, Ar-*H*), 7.48 (s, 1H, Ar-*H*). ^{13}C NMR (75 MHz, $CDCl_3$) (δ, ppm): 170.15, 161.17, 158.37, 136.04, 129.88, 128.05, 125.55, 101.88. LC-MS (*m/z*): 178.1 [M - COOH]$^-$, 222.1 [M - H]$^-$. IR (neat): 2858 1707, 1443, 1264 cm^{-1}.

*4.1.8. General synthesis of coupling of isoxazole acid with L-Ala-OCH_3 (**8a-c**)*

To the stirred solution of isoxazole acid (1.0 eq) in dry THF (5 mL/mmol) was added *N*,*N*-DIPEA (2 eq) and HATU (1.5 eq) and the reaction mixture was stirred at room temperature for 20 min. L-alanine methyl ester (1.1 eq) was added to the reaction mixture and was stirred at room temperature for 16 h. After completion of reaction, the reaction mixture was quenched with water and extracted with ethyl acetate. The combined organic layers were washed with brine solution, dried over anhyd. Na_2SO_4, filtered and concentrated under *vacuo*. The crude obtained was purified with column chromatography with 20% ethyl acetate in hexane to afford the title compound.

*4.1.8.1. (2R)-Methyl 2-(3-(5-bromo-3-methylbenzofuran-2-yl)isoxazole-5-carboxamido)propanoate (**8a**).* Brown solid, mp 160–162 °C, yield: 67%, R_f (hexane: ethyl acetate = 7:3): 0.63, ^{1}H NMR (400 MHz, $CDCl_3$) (δ, ppm): 7.73 (s, 1H, N*H*), 7.49–7.47 (m, 1H, Ar-*H*), 7.39–7.34 (m, 2H, Ar-*H*), 7.03 (s, 1H, Ar-*H*), 4.83–4.76 (m, 1H, C*H*), 3.79 (s, 3H, OCH_3), 2.53 (s, 3H, CH_3), 1.55 (s, 3H, CH_3).^{13}C NMR (75 MHz, $CDCl_3$) (δ, ppm): 172.55, 163.49, 158.25, 157.94, 153.38, 140.66, 131.41, 129.51, 123.08, 117.54, 116.42, 113.10, 101.20, 52.67, 48.25, 18.29, 8.62. LC-MS (*m/z*): $[M + 2H]^+$409.3. IR (neat): 3409, 2959, 1737, 1685, 1529, 1208 cm^{-1}.

*4.1.8.2. (2R)-methyl 2-(3-o-tolylisoxazole-5-carboxamido) propanoate (**8b**).* Creamish yellow solid, mp 68–70 °C, yield: 59%, R_f (hexane: ethyl acetate = 7:3): 0.64, ^{1}H NMR (400 MHz, DMSO-d_6) (δ, ppm): 9.22 (d, 1H, *J* = 6.84 Hz, N*H*), 7.76 (d, 1H, *J* = 7.36 Hz, Ar-*H*), 7.47–7.37 (m, 3H, Ar-*H*), 7.14 (s, 1H, Ar-*H*), 4.52 (q, 1H, *J* = 7.2 Hz,

CH), 3.66 (s, 3H, OCH$_3$), 2.49 (s, 3H, CH$_3$), 1.42 (d, 3H, $J = 7.2$ Hz, CH$_3$). ^{13}C NMR (75 MHz, $CDCl_3$) (δ, ppm): 172.63, 171.66, 158.59, 136.40, 131.48, 130.53, 128.48, 126.37, 102.19, 52.66, 48.17, 21.43, 18.31. LC-MS (m/z): 289.3 $[M + H]^+$. IR (neat): 3286, 3339, 1748, 1663 cm^{-1}.

*4.1.8.3. (R)-methyl 2-(3-(4-chlorophenyl) isoxazole-5-carboxamido) propanoate (**8c**).* Off-white solid, mp 144–146 °C, yield: 64%, R_f (hexane: ethyl acetate = 7:3): 0.55, ^{1}H NMR (300 MHz, $CDCl_3$) (δ, ppm): 7.73 (d, 2H, $J = 8.4$ Hz, Ar-H), 7.47 (d, 2H, $J = 8.4$ Hz, Ar-H), 7.34 (s, 1H, NH), 6.94 (s, 1H, Ar-H), 4.84–4.74 (m, 1H, CH), 3.80 (s, 3H, CH$_3$), 1.55 (t, 3H, $J = 7.2$ Hz, CH$_3$). ^{13}C NMR (75 MHz, $CDCl_3$) (δ, ppm): 171.60, 163.38, 161.54, 158.67, 135.24, 130.65, 129.65, 128.76, 101.88, 52.10, 49.5, 17.2. LC-MS: m/z $[M + H]^+$309.2. IR (neat): 3312, 1745, 1447 cm^{-1}.

*4.1.9. General synthesis of hydrolysis of isoxazole-Ala-OCH$_3$ (**9a-c**)*

To the stirred solution of isoxazole-Ala-OCH$_3$ (0.48 mmol) in the mixture of THF (6 mL) and water (2 mL) was added lithium hydroxide (2.2 eq) and the reaction mixture was stirred at room temperature for 4 h. After completion of reaction (monitored by TLC) the reaction mixture was concentrated under reduced pressure, added water, acidified with 1NHCl up to pH-2~3 and extracted with ethyl acetate (3 × 100 mL). The combined organic layer was washed with brine solution, dried over anhydrous Na_2SO_4, filtered and concentrated under reduced pressure to afford white acid.

*4.1.9.1. (2R)-2-(3-(5-bromo-3-methylbenzofuran-2-yl) isoxazole-5-carboxamido) propanoic acid (**9a**).* White soild, mp 201–203 °C (decomposed), yield: 74%, R_f(hexane: ethylacetate = 7: 3): 0.0, ^{1}H NMR (300 MHz, DMSO-d_6) (δ, ppm): 12.74 (brs, 1H, -COOH), 9.12 (d, 2H, $J = 6.9$ Hz, NH), 8.01 (d, 2H, $J = 7.8$ Hz, Ar-H), 7.65–7.56 (m, 2H, Ar-H), 7.32–7.27 (m, 2H, Ar-H), 4.45 (q, 1H, $J = 6.5$ Hz, CH), 2.49 (s, 3H, CH$_3$),1.31 (s, 3H, CH$_3$). ^{13}C NMR (75 MHz, $CDCl_3$) (δ, ppm): 173.81, 162.07, 159.26, 158.21, 153.21, 140.60, 131.55, 129.93, 123.92, 118.19, 116.40, 114.05, 102.05, 48.46, 17.15, 8.82. LC-MS: m/z $[M + H]^+$393.4.IR (neat): 3432, 1722, 1689, 1532, 1451 cm^{-1}.

*4.1.9.2. (R)-2-(3-(4-chlorophenyl) isoxazole-5-carboxamido) propanoic acid (**9b**).* White solid, mp177-179 °C (decomposed), yield: 70%, R_f (hexane: ethylacetate = 7: 3): 0.0, ^{1}H NMR (300 MHz, DMSO-d_6) (δ, ppm): 12.79 (brs, 1H, -COOH), 9.02 (d, 2H, $J = 7.5$ Hz, NH), 7.98 (d, 2H, $J = 8.4$ Hz, Ar-H), 7.64 (d, 2H, $J = 8.4$ Hz, Ar-H), 7.45 (s, 1H, Ar-H), 4.48 (q, 1H, $J = 7.2$ Hz, CH), 1.35 (s, 3H, CH$_3$). ^{13}C NMR (75 MHz, $CDCl_3$) (δ, ppm): 173.81, 169.78, 159.84, 158.69, 136.01, 129.90, 128.07, 125.60, 100.93, 48.37, 17.16.LC-MS: m/z $[M + H]^+$295.4.IR (neat): 3417, 3398, 3123, 1715, 1678, 1540, 1451, 1097 cm^{-1}

*4.1.9.3. 2-(3-(2-methylphenyl)isoxazole-5-carboxamido) propanoic acid (**9c**).* White solid, M.pt.: 146 °C, yield: 74%, R_f (hexane: ethylacetate = 7: 3): 0.0, ^{1}H NMR (400 MHz, DMSO-d_6) (δ, ppm): 7.72 (d, 1H, $J = 5.7$ Hz, NH), 7.39–7.38 (m, 2H, Ar-H), 7.33–7.30 (m, 2H, Ar-H), 6.88 (s, 1H, Ar-H), 4.38 (q, 1H, $J = 8.1$ Hz, CH), 2.51 (s, 3H, CH$_3$), 1.61 (d, 3H, $J = 5.4$ Hz, CH$_3$). ^{13}C NMR (75 MHz, $CDCl_3$) (δ, ppm): 176.63, 171.85, 158.95, 158.22, 136.46, 131.49, 130.59, 128.51, 126.37, 102.29, 48.16, 21.39, 17.94. LC-MS: m/z $[M + H]^+$275.5. IR (neat): 3361,3324, 1734, 1644, 1551, 1443, 1302 cm^{-1}.

4.2. X-ray crystallographic analysis

The structure of isoxazole acid (**7b**) was established by X-ray crystallographic analysis. Single crystal of the compound was obtained through the slow evaporation of its tetrahydrofuran solution. Suitable crystal was selected and analysed on an APEX II CCD Bruker diffractometer equipped with rotating anode generator, the radiation was monochromated with a Montel mirror (Cu Kα = 1.54178 Å). Intensity data were collected at 100 K using θ-scan method. No significant loss in intensities was observed during data collection. Multi-scan absorption corrections were applied to the intensity data empirically using SADABS [27]. Data collection, reduction and refinement were performed using APEX II [27] and SHELX [28] software. Crystal structures were solved by direct methods using SHELXS and refined with full-matrix least-squares based on F^2 using SHELXL [28]. All non-hydrogen atoms were refined anisotropically. Hydrogens were first located in the Fourier difference map, then positioned geometrically and allowed to ride on their respective parent atoms. The molecular graphics and crystallographic illustrations were prepared using *XP* [29].

4.3. Enzymatic inhibition assay

All compounds were dissolved in DMSO to a stock concentration of 10 mM. Initially the compounds were screened for inhibition with each of the four MetAP's (*Hs*MetAP1b, *Mt*MetAP1c, *Sp*MetAP1a, and *Ef*MetAP1a). Expression, purification and biochemical assays are performed as reported previously. The enzyme assays were performed using Met-AMC as substrate. % Inhibition were determined by using compound concentration range of 1 μM–120 μM. The *K*i values were determined by Dixon method. The reaction mixture contained 50 mM Hepes (pH-7.5 for *Sp*MetAP1a, *Ef*MetAP1a, *Mt*MetAP1c and pH-8.0 for *Hs*MetAP1b), 150 mM KCl, CoCl2 (3 M equivalents of the enzyme concentration), 4 μM enzymes (*Hs*MetAP1b, *Mt*MetAP1c, *Sp*MetAP1a or *Ef*MetAP1a) and 50, 100, 150 μM concentrations of L-Met-AMC. All reactions were performed in triplicate. 2,2′-Bipyridine was used as positive control [9,19].

4.4. Glide docking

In order to perform structure-function studies, docking of compounds **4a** and **5a** was carried out within the active sites of the methionine aminopeptidase from *M. tuberculosis* (PDB ID: 1YJ3), *E. faecalis* (PDB ID:3TB5) and *S. pneumoniae* (PDB ID: 4KM3) utilizing GLIDE5.8 [30] in extra precision (XP) mode as implemented in the Schrödinger Suite. During dockings, the receptors were kept rigid while ligands were treated as flexible, which enables to dock the ligand at the receptor's binding site.

The protein complexes were prepared using the protein-preparation wizard. Water molecules were eliminated as no water bridges observed in the complexes. After assignment of bond orders, polar hydrogens and adding missing residues, the whole systems were optimized to an RMSD of 0.30 Å. Subsequently, electron affinity grids were generated for each protein. Both the legands (**4a** and **5a**) were optimized and prepared using methods as mentioned in our earlier reports [31]. After ligand preparation, docking was performed using extra precision mode of GLIDE. To improve the geometry, post-docking minimization of the poses were accomplished.

4.5. In vitro antibacterial activity

The compounds which showed more than 60% enzyme inhibition (**2a-c**, **3a-b**, **4a-b**, **5a-b**, **6c** and **9a**) were screened for antibacterial activity against Gram-positive bacteria including *S. pneumoniae* (MTCC 655), *E. faecalis* (MTCC 439) and Gram-negative bacteria including *P. aurogenosa* (MTCC 2453), *S. typhimurium* (MTCC 3224), *K. pneumoniae* (ATCC 700603), *E. coli* (ATCC 25922) and multidrug resistant strains viz. *E. coli* MRA11 (GenBank Accession no. KJ957160), MRC17 (GenBank Accession no. KJ906623), MRC24 (GenBank Accession no. KM822765), MRAE26

(GenBank Accession no. KJ923014), MRAE32 (GenBank Accession no. KJ923017), MRAE33 (GenBank Accession no. KM822768), MRAE44 (GenBank Accession no. KJ923018) and MROB11 (GenBank Accession no. KC963018) using broth dilution technique according to standard protocol for antibacterial assessment by NCCLS [32]. Ciprofloxacin (CIP) was used as positive control. DMSO was used as solvent with less than 4% concentration in final volume used for the assay. The test compounds were serially diluted (1000–7.8 μg/mL) in 96 well plate containing (Tarson) 100 μL nutrient broth medium. Each well of plates was inoculated with 100 μL of fresh inoculums containing approximately 2.5×10^6 cells/mL and incubated at 37 °C with constant stirring of 150 rpm for 24 h. After incubation period, minimum inhibitory concentration (MIC) was determined as the lowest concentration of compound/drug at which no visible growth appeared.

However, in case of multi-drug resistant isolates, varying concentrations (8–1024 μg/mL for **4a** and **5a**) and (0.49–63.3 μg/mL for ciprofloxacin) were dispensed into a 96-well plate (Tarson) in luria broth medium. Then, the medium was inoculated with 10 μl of 1000 times diluted 0.1 OD_{600} culture and incubated overnight at 37 °C. The OD was measured at 600 nm using a microplate reader (Thermo Scientific MultiskanGo). Percentage inhibition of these resistant isolates was calculated using the formula:

Percentage inhibition = a−b a × 100.

Where a = pure culture reading − media reading.b = test reading − plain compound reading (if the compound is colored solution).

4.6. Synergistic study

Synergistic or antagonistic property of lead inhibitors **4a** and **5a** with standard drug ciprofloxacin was determined as fractional inhibitory concentration index (FICI) according to the checkerboard method [33]. A concentration gradient ranging from 1024 to 16 μg/mL of compounds **4a** and **5a** were maintained in 96 well plate followed by the addition of the ciprofloxacin with concentration ranging from 128 to 2 μg/mL in 100 μL of Mueller-Hinton broth. Then, 100 μL of a suspension of 5×10^5 CFU/mL was added in each well as inoculums incubated for 18 h at 37 °C. The fractional inhibitory concentration (FIC) index is defined as the sum of the MIC of each drug when used in combination divided by the MIC of the drug used alone. Synergy and antagonism were defined by FICI $\leq$0.5 and >4, respectively. Partially synergistic was denoted by 0.5 > FICI <1 while Indifferent was defined by 1 < FICI $\leq$4 [34].

4.7. Cytotoxicity by MTT assay

MTT (3-(4,5-dimethyl-2-yl)-2,5-diphenyl tetrazolium bromide), Dulbecco's modified Eagle's medium (DMEM), 0.25% trypsin and a 0.02% EDTA mixture were purchased from Hi Media (Mumbai, India). Fetal bovine serum (FBS) was obtained from Gibco (Grand Island, NY). The human embryonic kidney (HEK293) cell line was procured from National Centre for Cell Sciences (NCCS), Pune, India. The cells were cultured and maintained as a monolayer in DMEM supplemented with 10% FBS and antibiotics (100 units/mL penicillin and 100 μg/mL streptomycin) at 37 °C in humidified atmosphere of 5% CO_2 in T-25 flasks. The cells were subcultured twice in a week. A cell count of approximately 2×10^4 cells per well were seeded in 96-well plate (150 μL per well) and incubated for 24 h before treatment. The cells were then treated with varying concentrations (10–400 μg/mL) of the test compounds. After 48 h of incubation at 37 °C, the exhausted serum supplemented medium was removed and serum free media (50 μL) was added into each well. After that, 20 μL per well of MTT at a concentration of 5 mg/mL in PBS was added to each well and the plates were incubated for 4 h at 37 °C. Formazan crystals, the metabolized MTT product, were solubilized in DMSO (150 μL per well) and were quantified by reading the absorbance at 570 nm after incubation of 10 min on *iMark* Microplate Reader (Bio-Rad, Hercules, CA). All assays were performed in triplicate. Percent viability was taken as the relative absorbance of treated versus untreated control cells [35].

4.8. Growth kinetics studies

On the basis of preliminary studies and cytotoxicity, compound **5a** was selected as lead inhibitor and explored for further biological activities. Growth kinetics study of *S. pneumoniae* and *E. coli* was determined in the presence of lead inhibitors **5a** along with standard drug ciprofloxacin. 50 mL of sterile nutrient broth medium was inoculated with freshly prepared bacterial culture containing approx. 2×10^6 cells/mL. After addition of different concentrations (2MIC, MIC and ½ MIC) of compound **5a**, flasks were incubated at 37 °C and 160 rpm. Ciprofloxacin at a concentration of 10 μg/mL was used as positive control. Aliquots (1 mL) of culture were removed from each test sample at time interval of 2 h (*i.e.*, time point of 0, 2, 4, 6, 8, 10, 12, 14, 16, 18, 20 and 22 h) and growth was measured turbidometrically at 600 nm using Thermo MultiskanGo Spectrophotometer. Optical density was recorded for each concentration against time (h) [36].

4.9. Transmission electron microscopic (TEM) analysis

The morphology of *S. pneumoniae* and *E. coli* cells were analysed using TEM following the standard protocol [37]. Briefly, the cells were harvested, standardized ($A_{600} \approx 0.1$) and exposed to MIC conc. of test inhibitor **5a** for 1 h. Then, the cells were washed thrice with PBS to remove the residual medium and fixed overnight in 2.5% glutaraldehyde in phosphate/magnesium buffer (40 mM K_2HPO_4/KH_2PO_4, pH 6.5, 0.5 mM $MgCl_2$). The cells were washed twice for 15 min in 0.1 M sodium phosphate buffer (pH 6.0) and post-fixed for 2 h in 2% osmium tetroxide. Again, the cells were washed twice for 15 min in distilled water and then *en bloc* stained with 1% uranyl acetate (aqueous) for 30 min. After two further washes, cells were dehydrated in 95% and 100% ethanol. The cells were exposed to propylene oxide for 2 × 10 min and infiltrated for 1 h in 1:1 propylene/epoxy embedding material (Epon) mixture and then overnight in fresh Epon. After polymerization for 48 h at 60 °C, ultrathin sections were cut using a microtome (LeicaEM UC6) and transferred onto a copper grid. The samples were stained with uranyl acetate (saturated solution of uranyl acetate in 50% alcohol) followed by lead citrate. The samples were washed three times in Milli-Q (MQ) water and dried by touching with Whatman filter paper. The sections were examined with a Tecnai G2 20 high resolution transmission electron microscope (Fei Company, The Netherlands) at 200 kV.

4.10. Anti-biofilm assessment

Biofilm formation is an important virulence factor of most of the pathogenic micro-organism which is an initial step to establish an infection. Anti-biofilm activity of compound **5a** was determined by biochemical assay using XTT as well as by scanning electron microscopy (SEM).

4.10.1. Anti-biofilm activity by XTT assay

XTT (2, 3-bis (2-methoxy-4-nitro-5-sulphophenyl)-5-[(phenylamino) carbonyl]-2H-tetrazolium-hydroxide) reduction assay was used to determine the metabolic activity of biofilm formation in bacteria [38]. Compound **5a** was serially diluted with concentration

range from 1000 μg/mL to 7.8 μg/mL in microtitre plate having tryptic soy broth. Aliquots of 100 μL of tryptic soy broth containing bacterial inoculums of approximately 5×10^5 CFU/mL were added to each well and incubated at 37 °C for 24 h under static conditions. The medium was discarded and washed with phosphate buffer saline (PBS) to remove the non-adherent bacteria. To each well 50 μL of prepared XTT salt solution (HiMedia, INDIA) was added and plates were incubated at 37 °C in dark for 90 min. Bacterial dehydrogenase activity reduces XTT tetrazolium salt to XTT formazan, resulting in colorimetric change (turns to orange) that was correlated with cell viability. The colorimetric changes were measured spectrophotometrically at 490 nm [39]. The inhibition data were interpreted from dose–response curves, where an IC_{50} value is defined as the concentration of the inhibitor required to inhibit 50% of biofilm formation under the above assay conditions.

4.10.2. Scanning electron microscopic (SEM) analysis for biofilm formation

Scanning electron microscopic (SEM) analysis was performed to determine the biofilm formation by *E. coli using Sophisticated Analytical Instrumentation Facility (SAIF), AIIMS, New Delhi India.* The fresh bacterial cultures were prepared and inoculated into six-well cell culture plates containing 3 mL of tryptic soy broth (TSB) (containing 2.5 g/L of glucose). Glass coverslips (8 mm dia.) were dispensed into each well for biofilm formation on the surface and incubated at 37 °C for 24 h. Post incubation, plates were removed and the test compound was added to determine the anti-biofilm effect. Parafilm sealed plates were further incubated for the next 24 h. Coverslips were removed after total incubation of 24 h and washed with 0.1 M PBS. The biofilm that formed on the coverslips were placed in fixative (4%, v/v, formaldehyde in PBS) overnight. Samples were again washed with PBS and then coverslips were left for drying and later examined under scanning electron microscope [40].

4.11. In vivo toxicity evaluation of **5a** in G. mellonella larvae

The larvae of the sixth developmental stage of *G. mellonella* were obtained from the Meal Worm Company (Sheffield, England). The larvae of *G. mellonella* were stored in wood shavings in the dark at 15 °C prior to use. The larvae that were chosen for experiments weighed on 0.21 g and were used within 3–4 weeks of receipt. Ten healthy larvae were placed in sterile 9 cm Petri dishes with Whatman filter paper inserted inside. A culture of *E. coli* was grown to the stationary phase ($1–2 \times 10^8$/mL) in nutrient broth at 30 °C and 200 rpm. The cells were harvested by centrifugation (2056 g for 5 min on a Beckmann GS-6 bench centrifuge) washed in PBS and resuspended in PBS at a cell density 5×10^5 per 20 μL. The larvae were inoculated by injecting 20 μL through the last left pro-leg into the haemocoel using a Myjector syringe (Terumo Europe) and incubated for 1 h placed at 30 °C in the dark. After the incubation period, the larvae were inoculated with test compound **5a** at a concentrations of 2.5 mg suspended in PBS, supplemented with 12.5% DMSO (v/v), through the last right pro-leg. The larvae injected with 20 μL of PBS supplemented with 12.5% DMSO (v/v) were used as controls. For assessment of larval viability, the larvae were gently probed with a needle and if no response was observed, the larvae were considered to be dead.

Three larvae were inoculated with 20 μL of the compound **5a** solutions at concentration of 1.25 or 2.5 mg/mL. The larvae were then incubated at 30 °C, in the dark, for 24 h. The haemocyte density in the larvae was ascertained by piercing the backs of the anterior end ('head') of the three larvae with a sterile needle and collecting the yellow haemolymph ('blood'), ensuring no white floccular material was removed – this is the fat body and will impede counting. Haemolymph was diluted to 1 in 10 in cold PBS containing 0.37% (v/v) 2-mercaptoethanol to reduce clotting and melanisation. The solution was mixed gently by pipetting. Haemocytes were counted on a haemocytometer (0.0025 mm^2, Blau-Brand, Germany) and the density in the original larvae was calculated [41].

Acknowledgement

Mohammad Abid gratefully acknowledges the funding support in the form of Young Scientist from Science & Engineering Research Board (Grant No. SR/FT/LS-03/2011), New Delhi, INDIA and University Grant Commission (UGC), Govt. of India, for a RAMAN Postdoctoral Fellowship (F. no. 5-123/2016(IC)) to work at the Eppley Institute, UNMC, Omaha, NE, USA. BA and MI acknowledge BSR Meritorious fellowship and ICMR-RA Fellowship (3/2/3/15/2018/Online Onco Fship/NCD-III) for financial support, respectively.

Appendix A. Supplementary data

Supplementary data to this article can be found online at https://doi.org/10.1016/j.ejmech.2018.11.053.

References

[1] R.J. Fair, Y. Tor, Antibiotics and bacterial resistance in the 21st century, Perspect. Med. Chem. 6 (2014) 25–64.
[2] E.Y. Klein, T.P. Van Boeckel, E.M. Martinez, S. Pant, S. Gandra, S.A. Levin, H. Goossens, R. Laxminarayan, Global increase and geographic convergence in antibiotic consumption between 2000 and 2015, Proc. Natl. Acad. Sci. Unit. States Am. 115 (15) (2018) E3463–E3470.
[3] https://www.cdc.gov/drugresistance/index.html.
[4] S.E. Rossiter, M.H. Fletcher, W.M. Wuest, Natural products as platforms to overcome antibiotic resistance, Chem. Rev. 117 (2017) 12415–12474.
[5] W.L. Wang, S.C. Chai, Q.Z. Ye, Synthesis and structure-function analysis of Fe (II)-form-selective antibacterial inhibitors of *Escherichia coli* methionine aminopeptidase, Bioorg. Med. Chem. Lett 19 (4) (2009) 1080–1083.
[6] M. Huang, S.X. Xie, Z.Q. Ma, R.P. Hanzlik, Q.Z. Ye, Metal mediated inhibition of methionine aminopeptidase by quinolinyl sulfonamides, Biochem. Biophys. Res. Commun. 339 (2) (2006) 506–513.
[7] R.A. Bradshaw, W.W. Brickey, K.W. Walker, N-terminal processing: the methionine aminopeptidase and N alpha-acetyl transferase families, Trends Biochem. Sci. 23 (1998) 263–267.
[8] M.D. Vaughan, P.B. Sampson, J.F. Honek, Methionine in and out of proteins: targets for drug design, Curr. Med. Chem. 9 (3) (2002) 385–409.
[9] C. Kishor, T. Arya, R. Reddi, X. Chen, V. Saddanapu, A.K. Marapaka, A. Addlagatta, Identification, biochemical and structural evaluation of species-specific inhibitors against type I methionine aminopeptidases, J. Med. Chem. 56 (13) (2013) 5295–5305.
[10] C.G. Miller, A.M. Kukral, J.L. Miller, N.R. Movva, pepM is an essential gene in *Salmonella typhimurium*, J. Bacteriol. 171 (1989) 5215–5217.
[11] S.Y. Chang, E.C. McGary, S. Chang, Methionine aminopeptidase gene of *Escherichia coli* is essential for cell growth, J. Bacteriol. 171 (1998) 4071–4072.
[12] S.S. Narayanan, K.M. Nampoothiri, Biochemical characterization of recombinant methionine aminopeptidases (MAPs) from *Mycobacterium tuberculosis* H37Rv, Mol. Cell. Biochem. 365 (2012) 191–202.
[13] C. Fossey, N.T. Huynh, A.H. Vu, A. Vidu, I. Zarafu, D. Laduree, A.M. Aubertin, Synthesis and anti-HIV evaluation of hybrid-type prodrugs conjugating HIV integrase inhibitors with d4t by self-cleavable spacers containing an amino acid residue, J. Enzym. Inhib. Med. Chem. 22 (5) (2007) 608–619.
[14] C.A. Shaw-Reid, V. Munshi, P. Graham, A. Wolfe, M. Witmer, R. Danzeisen, D.B. Olsen, S.S. Carroll, M. Embrey, J.S. Wai, M.D. Miller, Inhibition of HIV-1 ribonuclease H by a novel diketo acid, 4-[5-(benzoylamino) thien-2-yl]-2, 4-dioxobutanoic acid, J. Biol. Chem. 278 (5) (2003) 2777–2780.
[15] A. Stevaert, R. Dallocchio, A. Dessì, N. Pala, D. Rogolino, M. Sechi, L. Naesens, Mutational analysis of the binding pockets of the diketo acid inhibitor L-742,001 in the influenza virus PA endonuclease, J. Virol. 87 (19) (2013) 10524–10538.
[16] V. Summa, A. Petrocchi, P. Pace, V.G. Matassa, R. De Francesco, S. Altamura, L. Tomei, U. Koch, P. Neuner, Discovery of α, γ-diketo acids as potent selective and reversible inhibitors of hepatitis C virus NS5b RNA-dependent RNA polymerase, J. Med. Chem. 47 (1) (2004) 14–17.
[17] A. Bacchi, M. Carcelli, C. Compari, E. Fisicaro, N. Pala, G. Rispoli, D. Rogolino, T.W. Sanchez, M. Sechi, V. Sinisi, N. Neamati, Investigating the role of metal chelation in HIV-1 integrase strand transfer inhibitors, J. Med. Chem. 54 (24) (2011) 8407–8420.
[18] T. Arya, R. Reddi, C. Kishor, R.J. Ganji, S. Bhukya, R. Gumpena, S. McGowan,

M. Drag, A. Addlagatta, Identification of the molecular basis of inhibitor selectivity between the human and streptococcal type I methionine aminopeptidases, J. Med. Chem. 58 (5) (2015) 2350–2357.
[19] M.M. Masood, V.K. Pillalamarri, M. Irfan, B. Aneja, M.A. Jairajpuri, M. Zafaryab, M.M.A. Rizvi, U. Yadava, A. Addlagatta, M. Abid, Diketo acids and their amino acid/dipeptidic analogues as promising scaffolds for the development of bacterial methionine aminopeptidase inhibitors, RSC Adv. 5 (43) (2015) 34173–34183.
[20] P. Hasan, B. Aneja, M.M. Masood, M.B. Ahmad, U. Yadava, C.G. Daniliuc, M. Abid, Efficient synthesis of novel N-substituted 2-carboxy-4-quinolones via lithium bis (trimethylsilyl) amide (LiHMDS)-induced in situ cyclo-condensation reaction, RSC Adv. 7 (19) (2017) 11367–11372.
[21] S.C. Chai, W.L. Wang, D.R. Ding, Q.Z. Ye, Growth inhibition of *Escherichia coli* and methicillin-resistant *Staphylococcus aureus* by targeting cellular methionine aminopeptidase, Eur. J. Med. Chem. 46 (8) (2011) 3537–3540.
[22] A.W. Burgstahler, L.R. Worden, Coumarone, Org. Synth. 46 (1966), 28-28.
[23] C.H. Wu, M.S. Hung, J.S. Song, T.K. Yeh, M.C. Chou, C.M. Chu, J.J. Jan, M.T. Hsieh, S.L. Tseng, C.P. Chang, W.P. Hsieh, Discovery of 2-[5-(4-Chloro-phenyl)-1-(2, 4-dichloro-phenyl)-4-ethyl-1 H-pyrazol-3-yl]-1, 5, 5-trimethyl-1, 5-dihydro-imidazole-4-thione (BPR-890) via an active metabolite. A novel, potent and selective cannabinoid-1 receptor inverse agonist with high antiobesity efficacy in DIO mice, J. Med. Chem. 52 (14) (2009) 4496–4510.
[24] N. Patel, L. Chu, R. Chidambaram, J. Zhu, J. Kant, Enantioselective microbial reduction of 2-oxo-2-(1′, 2′, 3′, 4′-tetrahydro-1′, 1′, 4′, 4′-tetramethyl-6′-naphthalenyl) acetic acid and its ethyl ester, Tetrahedron: Asymmetry 13 (4) (2002) 349–355.
[25] S.P. Chakrabarty, R. Ramapanicker, R. Mishra, S. Chandrasekaran, H. Balaram, Development and characterization of lysine based tripeptide analogues as inhibitors of Sir2 activity, Bioorganic Med. Chem. 17 (23) (2009) 8060–8072.
[26] M. Sechi, G. Angotzi, R. Dallocchio, A. Dessì, F. Carta, L. Sannia, A. Mariani, S. Fiori, T. Sanchez, L. Movsessian, C. Plasencia, Design and synthesis of novel dihydroxyindole-2-carboxylic acids as HIV-1 integrase inhibitors, Antivir. Chem. Chemother. 15 (2) (2004) 67–81.
[27] APEX2, *SAINT* (2013) and *SADABS* (2014, Bruker AXS Inc., Madison, Wisconsin, USA, 2014.
[28] G.M. Sheldrick, Acta Crystallogr. A64 (2014) 112–122.
[29] XP – Interactive molecular graphics, Version 5.1, Bruker AXS Inc., Madison, Wisconsin, USA, 1998.
[30] U. Yadava, M. Singh, M. Roychoudhury, Pyrazolo [3, 4-d] pyrimidines as inhibitor of anti-coagulation and inflammation activities of phospholipase A 2: insight from molecular docking studies, J. Biol. Phys. 39 (3) (2013) 419–438.
[31] U. Yadava, B.K. Shukla, M. Roychoudhury, D. Kumar, Pyrazolo [3, 4-d] pyrimidines as novel inhibitors of O-acetyl-l-serine sulfhydrylase of Entamoeba histolytica: an in silico study, J. Mol. Model. 21 (4) (2015) 96.
[32] W.A. Wikler, Performance Standards for Antimicrobial Susceptibility Testing: Seventeenth Informational Supplement, Clinical and Laboratory Standards Institute (CLSI), 2007.
[33] M.B. Marques, E.S. Brookings, S.A. Moser, P.B. Sonke, K.B. Waites, Comparative *in vitro* antimicrobial susceptibilities of nosocomial isolates of *Acinetobacter baumannii* and synergistic activities of nine antimicrobial combinations, Antimicrob. Agents Chemother. 41 (1997) 881–885.
[34] M. Irfan, B. Aneja, U. Yadava, S.I. Khan, N. Manzoor, C.G. Daniliuc, M. Abid, Synthesis, QSAR and anticandidal evaluation of 1,2,3-triazoles derived from naturally bioactive scaffolds, Eur. J. Med. Chem. 93 (2015) 246–254.
[35] B. Aneja, M. Irfan, C. Kapil, M.A. Jairajpuri, R. Maguire, K. Kavanagh, M.M.A. Rizvi, N. Manzoor, A. Azam, M. Abid, Effect of novel triazole–amino acid hybrids on growth and virulence of *Candida* species: *in vitro* and *in vivo* studies, Org. Biomol. Chem. 14 (2016) 10599–10619.
[36] K. Theophel, V.J. Schacht, M. Schlüter, S. Schnell, C.S. Stingu, R. Schaumann, M. Bunge, The importance of growth kinetic analysis in determining bacterial susceptibility against antibiotics and silver nanoparticles, Front. Microbiol. 5 (2014) 544.
[37] M. Irfan, S. Alam, N. Manzoor, M. Abid, Effect of quinoline based 1,2,3-triazole and its structural analogues on growth and virulence attributes of *Candida albicans*, PloS One 12 (2016) e0175710.
[38] P.J. Baker, Regulation of the magnitude of the antibody response to bacterial polysaccharide antigens by thymus-derived lymphocytes, Infect. Immun. 58 (1990) 3465–3468.
[39] M.D. Felton, G. Kauffmam, B. Prescott, B. Ottinger, Studies on the mechanism of immunological paralysis induced in mice by pneumococcal polysaccharides, J. Immunol. 74 (1955) 17–26.
[40] V. Antoci Jr., C.S. Adams, J. Parvizi, H.M. Davidson, R.J. Composto, T.A. Freeman, E. Wickstrom, P. Ducheyne, D. Jungkind, I.M. Shapiro, N.J. Hickok, The inhibition of *Staphylococcus epidermidis* biofilm formation by vancomycin-modified titanium alloy and implications for the treatment of periprosthetic infection, Biomaterials 29 (2008) 4684–4690.
[41] B. Aneja, M. Azam, S. Alam, A. Perwez, R. Maguire, U. Yadava, K. Kavanagh, C.G. Daniliuc, M.M.A. Rizvi, Q.M.R. Haq, M. Abid, Natural product-based 1, 2, 3-triazole/sulfonate analogues as potential chemotherapeutic agents for bacterial infections, ACS Omega 3 (6) (2018) 6912–6930.